Journal of Applied Physics

REVIEW ARTICLE | JANUARY 08 2025

Compositional disordering: Nanoscale engineering of advanced crystalline scintillation materials

Special Collection: Disordered Materials at the Atomic Scale

M. Korzhik; V. Retivov; V. Dubov; V. Ivanov; I. Komendo; D. Lelekova; P. Karpyuk; V. Mechinsky; A. Postupaeva; V. Smyslova; V. Shlegel; I. Shpinkov; A. Vasil'ev

J. Appl. Phys. 137, 020701 (2025)
https://doi.org/10.1063/5.0238695

Journal of
Applied Physics

REVIEW

pubs.aip.org/aip/jap

Compositional disordering: Nanoscale engineering of advanced crystalline scintillation materials

Cite as: J. Appl. Phys. **137**, 020701 (2025); doi: 10.1063/5.0238695
Submitted: 13 September 2024 · Accepted: 14 December 2024 ·
Published Online: 8 January 2025

View Online Export Citation CrossMark

M. Korzhik,[1,2,a)] V. Retivov,[1] V. Dubov,[1] V. Ivanov,[3] I. Komendo,[1] D. Lelekova,[1] P. Karpyuk,[1] V. Mechinsky,[1,2] A. Postupaeva,[4] V. Smyslova,[1] V. Shlegel,[5] I. Shpinkov,[6] and A. Vasil'ev[6,a)]

AFFILIATIONS

[1]NRC Kurchatov Institute, Moscow, Russia
[2]Institute for Nuclear Problems, Belarus State University, Minsk, Belarus
[3]Kurnakov Institute of General and Inorganic Chemistry RAS, Moscow, Russia
[4]Crystal Manufacturing Lab, LTD, Novosibirsk, Russia
[5]Nikolaev Institute of Inorganic Chemistry SB RAS, Novosibirsk, Russia
[6]Skobeltsyn Institute of Nuclear Physics, Lomonosov Moscow State University, Moscow, Russia

Note: This paper is part of the special topic on Disordered Materials at the Atomic Scale.
[a)]**Authors to whom correspondence should be addressed:** mikhail.korjik@cern.ch and anv@sinp.msu.ru

ABSTRACT

This article provides an overview of the latest results in the field of improving the properties of multiatomic inorganic oxide compounds for scintillators. A possibility to control the spatial distribution of nonequilibrium carriers in the ionization track by creating a compositional disorder in the crystalline matrix is in focus. Managing the disorder at the nanoscale level creates an opportunity for the efficient energy loss by carriers during thermalization, smaller spatial dispersion, and, consequently, more efficient binding into excitons and, further, an increase in the scintillation yield. The methods to produce multicationic crystalline scintillation materials have been discussed. The effectiveness of the approach is confirmed for both activated and self-activated scintillation materials.

I. INTRODUCTION

Nowadays, in the field of the research and development of the materials for photonics, there is a tendency to produce and evaluate more complex systems that generate optical photons: crystalline materials,[1–4] organic composites,[5,6] metal-organic systems,[7] and nano-sized luminescence objects built into various matrices.[8] Apparently, it is tricky to categorize that simple crystalline systems have exhausted the potential for improvement, but they do not provide wide opportunities for manipulating their luminescent properties. Most of them quite rarely provide the possibility of targeted adjustment of the properties of materials of the same structural type and similar composition for use in different devices utilizing the generation of optical photons. Designing the materials, which accounts for a number of applications, significantly reduces the costs and is highly demanding. Among a variety of materials for photonics, oxide crystalline compounds are of particular interest. They are highly manufacturable and are widely used to obtain laser properties due to the stimulated luminescence[9] or to produce photons in a wide spectral range due to spontaneous luminescence under various types of excitations.[10–13] The excitation of luminescence by ionizing radiation in such materials, that is, scintillation and cathodoluminescence, is increasingly used, especially in imaging and diagnostic systems, radiography, and scientific research.[14–20] As a rule, such materials are subject to a special requirement: radiation resistance[21] of scintillation parameters when operating in an ionizing radiation environment. In just over a century of development of scintillation materials, it has been possible to reliably identify several structural types of oxide compounds that are resistant to irradiation with various types of ionizing radiation.[22–28] These are crystalline materials of the garnet structural type based on trivalent cations, orthosilicate compounds combining three- and four-charged cations, as well as tungstate compounds of the scheelite structural type, including two- and six-charged cations. All the above structural types of materials allow isovalent and non-isovalent doping, but more importantly, they form a variety of solid solutions with isostructural substitution. The latter ability makes it possible to adjust and improve the features of crystalline compounds of these structural classes for use as scintillation materials. Recently, reviews on the topic have been published.[29,30] The authors analyzed the use of increasing the complexity of the composition of the cationic and anionic sublattices in crystalline compounds suitable for detecting ionizing radiation to improve primarily the scintillation yield. Over the past two years, significant achievements have been made, in both experimental results and further development of the theory and capabilities for modeling the processes leading to the formation of an ensemble of luminescent centers after excitation by ionizing radiation.[31–42] To date, a significant improvement in the scintillation yield was found in many crystalline compounds with different activating ions; recently, it has been confirmed in the mixed self-activated scintillators[43] as well.

In this review, we focused on analyzing the physical and physico-chemical principles for the improvement in scintillation parameters with increasing complexity of the cationic composition of a compound, as well as considering changes in the properties of specific compounds when manipulating their cationic composition. The conclusions are supported by Monte Carlo simulations, electron microscopy data, and measurements of photoluminescence and scintillation properties.

Section II describes the general issues related to the features of the scintillation process development in crystalline systems with compositional disorder, as well as the issues of Frenkel excitons transfer along the diluted gadolinium sublattice. Section III is devoted to the technological capabilities to produce various multicationic oxide scintillation materials, with a focus on the production of transparent ceramics of the garnet structural type and the results of their properties evaluation. Finally, Sec. IV considers the limits of the approach and prospects for the next materials, for which compositional engineering can be useful in terms of improving scintillation characteristics. Section V concludes the study.

II. EFFECT OF COMPOSITIONAL DISORDER ON THE INTERACTION OF CRYSTALLINE SYSTEMS WITH IONIZING RADIATION

A. Control of ionization track parameters

In most cases, the interaction of ionizing radiation with the medium results in the ionization of the inner shells of the ions that form it. A random track of nonequilibrium carriers appears. The spatial distribution of thermalized nonequilibrium carriers determines the efficiency of transfer of electronic excitation energy to the ensemble of radiative centers.[44] Since the excitation of luminescent centers, as a rule, in oxide compounds includes the stage of formation of excitonic states,[45] it is obvious that the final scintillation yield is determined by the concentration of excitons in the track. Therefore, material engineering at the nanoscale to achieve track parameters that promote the most efficient formation of exciton states from thermalized nonequilibrium carriers is one of the priorities. It is important to note that the high ionization density in the track, which occurs when heavy charged particles, alpha particles, tritons, or fragments of nuclei are decelerated in matter, leads to the concentration quenching of excitons, which, as was also noted by Birks,[46] leads to a decrease in the yield scintillation. The light yield under charged particles depends on the chemical composition of the material as well.[47]

Mixing of cations in the matrix by isovalent and isostructural substitution is characterized by a random distribution of cations in the corresponding sublattice; thus, compositional disorder occurs. By such a substitution, there is no change in the structural type of the compound nor a decrease in the space group of symmetry of the crystal lattice; that is, crystallinity is preserved. When mixing cations, the anion sublattice is responsible for maintaining long-range order in the arrangement of ions in the lattice and, accordingly, vice versa. At the same time, introducing compositional disorder into the cation sublattice leads to a significant change in the distribution of the density of electronic states near the top of the bandgap. The difference in the formation of the landscape of the bottom of the conduction band can be revealed by considering fluctuations of the effective potential in a supercell consisting of hundreds of primitive cells of a mixed crystal with a random distribution of cations. Fluctuations of the effective potential in the one-electron approximation of the lower branch in the conduction band of the crystal, causing scattering of electronic states, can be constructed by the pseudopotential method according to the model.[48] A two-dimensional cross section of the spatial distribution of the pseudopotential $u(\vec{r})$ binary compounds $Y_3Al_5O_{12}$ and $Y_3Ga_5O_{12}$, as well as ternary compounds consisting of an equimolar ratio of $Y_3Al_5O_{12}$ и $Y_3Ga_5O_{12}$ is shown in Fig. 1. The spatial distribution of substituting ions was chosen to be uniform, without clustering. 2D sections are constructed in supercells $15 \times 15 \times 15$ at $z = \frac{15}{2}(\vec{a} + \vec{b} + \vec{c})_z$, i.e., at half their height. The unit cell

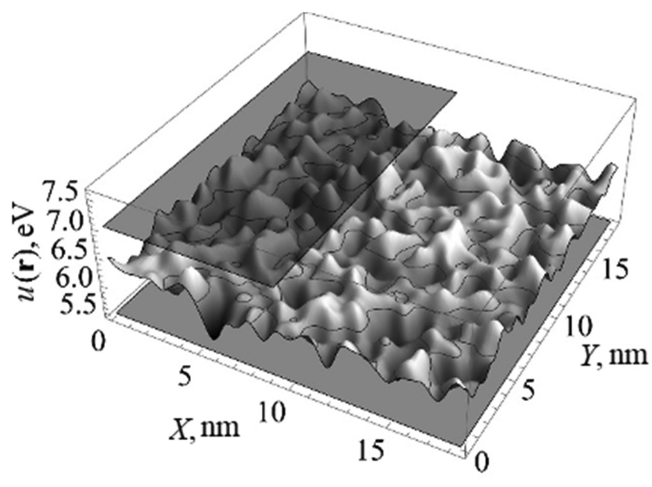

FIG. 1. Two-dimensional sections of the spatial distribution of the pseudopotential $u(\vec{r})$: $Y_3Al_5O_{12}$ (upper plane, $E_g = 7.01$ eV), $Y_3Ga_5O_{12}$ (lower plane, $E_g = 5.46$ eV), and $Y_3(Al,Ga)_5O_{12}$ between them.

parameters of the binary garnet compounds, the position of ions in the unit cell, and the bandgaps were taken from Ref. 49.

The amplitude of pseudopotential fluctuations in a ternary compound is determined by the difference in the bandgaps of binary compounds. As seen, it reaches fairly large values in a ternary system consisting of Al^{3+} and Ga^{3+} ions. In contrast, in compounds where heavier cations such as Y and Lu are mixed, the modulation is not as great since the end compounds $Lu_3Al_5O_{12}$ and $Y_3Al_5O_{12}$ have bandgap values of Eg = 7.61 and 7.01 eV, respectively. The same situation is observed in compounds with an orthosilicate structure when lutetium and yttrium are mixed, since bandgap values of Lu_2SiO_5 (LSO) and Y_2SiO_5 also differ a little; they are Eg = 7.27 and 7.38 eV, respectively.

The effect of modulation of the effective potential in a compositionally disordered crystal on the mobility of nonequilibrium carriers can be divided into two processes: first, an elastic scattering of free carriers with kinetic energy above the localization threshold on potential fluctuations and next, a localization of thermalized carriers in potential wells due to the modulation of the bottom of the conduction band with the possibility of subsequent activation due to phonon absorption. When the known relationships between the spatial dimensions of potential fluctuations and their depth are satisfied, electronic states appear that form a tail of the density of states. Such localization with wave functions spread over several ions can be regarded as the appearance of shallow traps induced either by compositional disorder or defects of different origins (intrinsic or extrinsic), which can be especially important in mixed systems. The appearance of tails of density of states results in the modification of the character of mobility of carriers up to hopping motion. In both processes, the modulation of the effective potential leads to a decrease in the diffusion scattering length of free carriers, an increase in the concentration of bound electron–hole pairs, and, consequently, an increase in the efficiency of the transfer of electronic excitations to luminescence centers.

Figure 2 shows random ionization tracks calculated using the LEPAM software package[50] in a Lu_2SiO_5 (LSO) crystal, which appears instantly after the photo-absorption of a gamma-quantum with an energy of 100 keV followed by the cascade of production of secondary excitations and after the thermalization of carriers in the track.

Figure 3 shows the distribution over distances between thermalized carriers, holes, and electrons in crystalline compounds of Lu_2SiO_5 and $(Lu,Y)_2SiO_5$ (LYSO). As seen, the average value of the distribution in $(Lu,Y)_2SiO_5$ is closer to the Onsager radius, which causes more effective coupling of the carriers into the pairs.

Note that disorder in the cation sublattice begins to affect the spatial distribution of carriers already at the stage of their thermalization. This occurs both as a result of scattering on inhomogeneities of the crystal potential and due to the excitation of phonons localized in these potential wells formed by inhomogeneities. When electrons are thermalized and have insignificant kinetic energy, they can also be captured by shallow traps based on inhomogeneities and lead to a delay in scintillation or even phosphorescence.[51] The influence of such defects is eliminated by introducing a small concentration of aliovalent codoping ions into the material, which create a center with a relatively deep location relative to the bottom of the conduction band and a high probability of nonradiative relaxation.[52–54]

B. Electronic excitation transport control by changing the integrity of the gadolinium sublattice in activated scintillators

Gadolinium-containing scintillators are very attractive from the point of view of controlling the scintillation properties as well as managing the sensitivity to various types of ionizing radiations.[55–58] In contrast to the crystals based on Y, La, and Lu, which have no peculiarities of the electron density states into the bandgap, the Gd^{3+}-based crystal host has numerous f-levels (^6P, ^6I, ^6D) creating sub-zones. Moreover, following the extended Dieke diagram,[59] one can suppose that numerous Gd^{3+} levels in the energy range above 40 000 cm^{-1} will provide a chain of consecutive processes that include effective capture of nonequilibrium carriers by Gd ions and intracenter relaxation to the lowest states (^6P, ^6I). The intracenter relaxation process is quite short and proceeds within a picosecond.[60] So, besides the lattice self-trapped excitons (STEs) having energy slightly less than the bandgap energy, a significant part of nonequilibrium carriers create Frenkel-type excitons (FTEs), which have a capability for migration along with ^6P, ^6I, and ^8S states of the Gd^{3+} sublattice. The increase in the compositional disorder due to the dilution of the gadolinium sublattice, i.e., the transition from ternary to quaternary and then quintuple compounds, inevitably leads to a violation of the integrity of the gadolinium sublattice. Typically, an interaction associated with the excited Gd^{3+} $5d^04f^7$ configuration and Ce^{3+} activating ions is described by the dipole–dipole interaction energy transfer. At the same time, diffusion over the *f*-states of gadolinium by hopping occurs due to the dipole–dipole transfer as well. Therefore, the energy transfer process is a diffusion-controlled dipole–dipole transfer. In addition, $Gd^{3+} \rightarrow Ce^{3+}$ the exchange (Dexter) transfer occurs as well.

Let us consider two cases of the change in the composition of $Gd_3Al_2Ga_3O_{12}$:Ce (GAGG:Ce): when gadolinium ions are partly substituted by lightweight or heavy cations. Mixing of cations influences the ionization process. When diluted by light yttrium cations, the photoabsorption and ionization still dominate near heavier gadolinium atoms. On the contrary, when the gadolinium sublattice is diluted by heavier lutetium cations, a significant part of photoabsorption and ionization are localized on these heavy ions. Therefore, in the first case, FTE will dominate in the excitation transfer to Ce^{3+} ions, while in the latter case, STE will make a significant contribution. A Monte Carlo simulation of the transfer processes at the conditions of the migration of excitations along the Gd sublattice with the broken integrity was performed in Ref. 36. The incorporation of Lu ions into the Gd sublattice leads to a deceleration of the transformation of STE into mobile FTE. Figure 4 depicts the results of a simulation of the contribution of different transfer mechanisms to the Ce^{3+} ions from the Gd sublattice and STE and the resulting luminescence kinetics at a few concentrations of Ce^{3+} ions in GAGG:Ce and $(Gd,Lu)_3Al_2Ga_3O_{12}$:Ce (GLAGG:Ce). Typically, GAGG:Ce has two major components in the scintillation kinetics, and their decay constants show a reduction with increasing Ce concentration in the compound. In the compound with the Gd sublattice diluted by Lu ions, the fraction of both scintillation kinetic

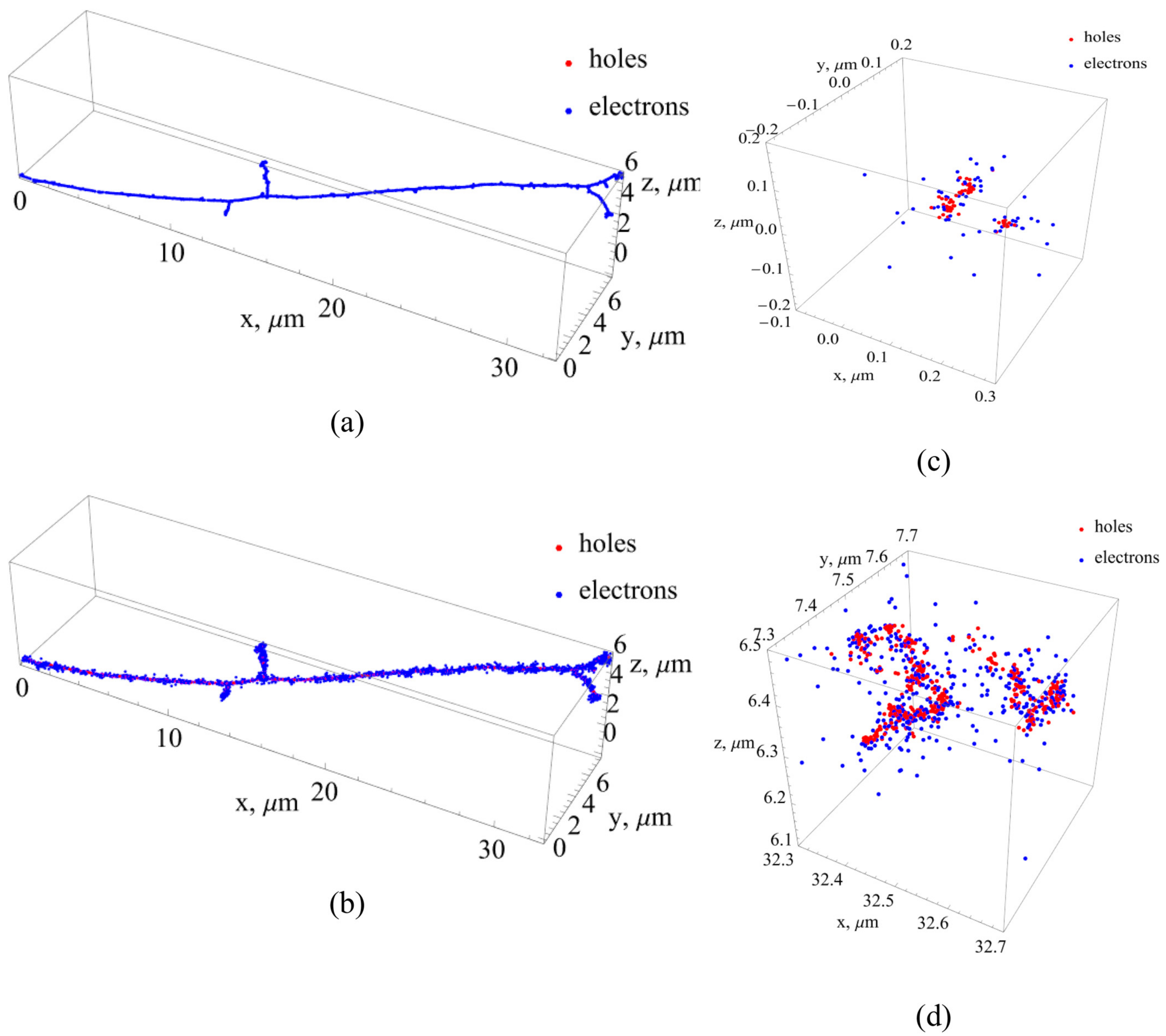

FIG. 2. A random ionization track in a Lu_2SiO_5 crystal after the photo-absorption of a gamma-quantum with an energy of 100 keV that appears instantly (a) and after thermalization of nonequilibrium carriers (b). A magnified fragment of the spatial distribution of thermalized carriers at the beginning of the track (c) and at the end of the track (d). Holes are denoted as red dots and electrons are denoted as blue dots.

components is a little dependent on the Ce concentration. Therefore, slow scintillation kinetics is observed, and it is hardly removable.[61,62]

Moreover, the diminished role of the Gd subsystem in the delivery of electronic excitations to Ce^{3+} ions causes a drop in LY. Worth noting, when Gd is completely removed from the crystal matrix, the ternary Lu–Al–Ga garnet demonstrates LY at the level of YAG or even worse.[63]

III. STATE-OF-ART OF THE PRODUCTION AND EVALUATION OF COMPOSITIOLALLY DISORDERED OXIDE SCINTILLATORS

A. Production of crystalline multiatomic compounds with compositional disorder

High-quality multi-cationic crystalline compounds are quite difficult to obtain by pulling from the melt due to the difference

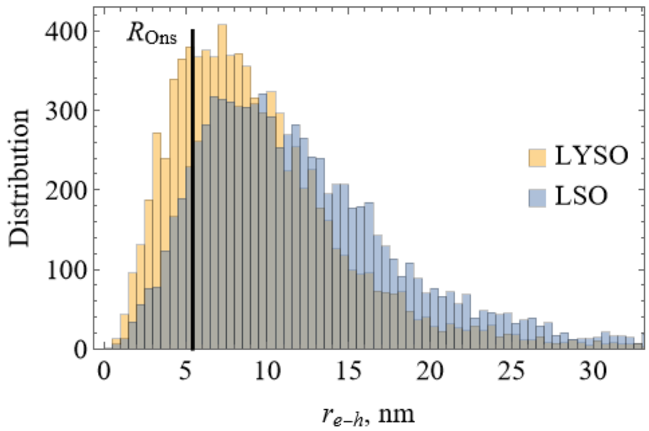

FIG. 3. Distribution of distances between holes and the nearest electron for LYSO and LSO (assuming 1.5 times larger thermalization length), R_{Ons} is the Onsager radius (within an e–h pair directly converted into the exciton).

in the pressure of saturated vapors in the growth chamber of various components. Moreover, a gradient of various cations along the growth axis is expected to occur. An alternative method for producing the crystalline compound is the production of ceramics without melting. This method is effective for compounds with a cubic space symmetry group, which narrows the list of potentially suitable compounds. Ceramic production includes several successive technological processes, which can be summarized as three stages: powder production of a specified composition and particles dimensions, compaction, and sintering.

B. Production of precursors

The commonly used method to produce precursors for manufacturing the ceramics of garnet structural-type compounds is solid-phase synthesis. It is widely used for three- and four-cation compositions.[64] The mixing of oxide powders in ball mills is carried out for several tens of hours, and then, annealing at temperatures above 1000 °C is applied. The advantages of the method are its simplicity, availability, and scalability, while the result of the process significantly depends on the microstructure of the starting powders and the size of their particles. At the same time, long-term grinding requires careful selection of the material of the grinding bodies and the lining of the drum to minimize their abrasion and contamination of the target powders. Certain difficulties may arise in the presence of easily evaporated components in the mixture, for example, gallium oxide.[65]

The next useful method is spray pyrolysis, which is the process of spraying a solution containing metal cations into a tube furnace or flame. The major feature of the method is the production of particles of a regular spherical shape with a narrow size distribution using a solution of metal salts: alcoholates and carboxylates. The disadvantages of the method are technological difficulties, the high cost of pyrolysis setup, and low productivity.[66,67] In addition, the production of ceramics from powders with spherical particles requires the application of pressure during sintering due to the small area of their contact with each other. Moreover, spherical particles can be hollow inside, which complicates the production of ceramics even under hot pressing conditions.

The solgel method, suitable for obtaining nanoscale oxides, includes four stages: the fabrication of a sol, concentrating with subsequent gelation, drying the gel to remove the solvent, and heat treatment to obtain the target phase. In the case of the production of nanosized powders of rare earth garnets, the original

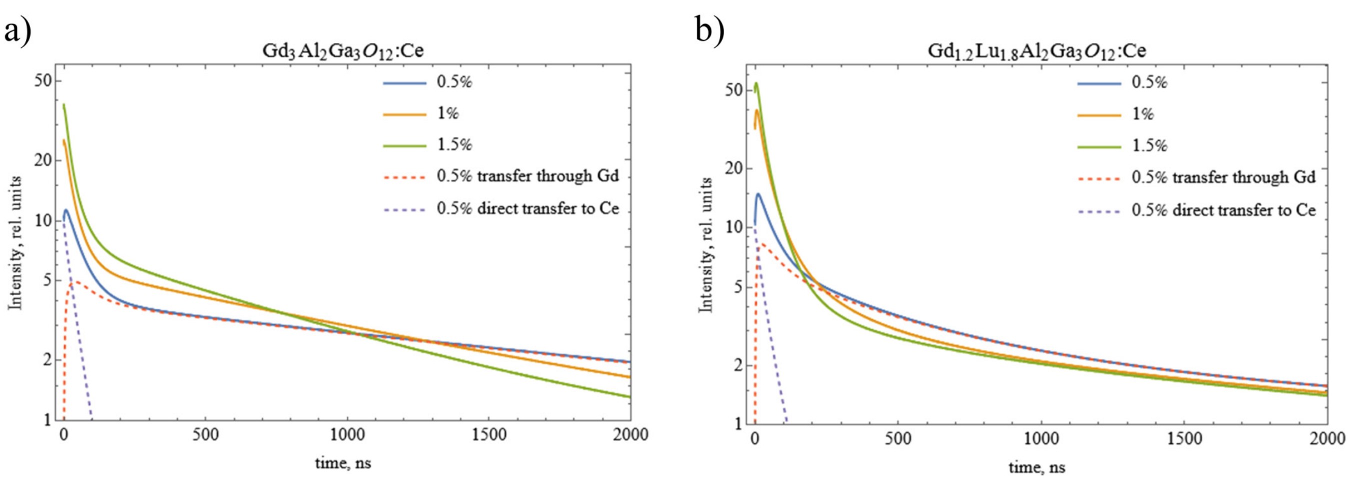

FIG. 4. Simulation of scintillation kinetics of GAGG (a) and GLAGG (b) on the Ce concentration (indicated). Dashed curves show a contribution of the mechanisms of the electronic excitations transfer via Gd sublattice and direct transfer from STE at a Ce concentration of 0.5 at. %. The integrals under kinetics are the same as in Ref. 36 [Korzhik *et al.*, Crystals **12**(9), 1196 (2022), licensed under a Creative Commons Attribution CC BY 4.0 license].

components are converted into a solution. Next, an organic reagent (e.g., ethylene glycol, citric acid, 1,2-ethanediol) is usually added to the solution, and the latter is gradually evaporated (at a temperature of about 80 °C) to form a sol, which, upon further evaporation of the solvent, loses its aggregative stability and turns into a gel. The obtained gel is dried at temperatures of 90–110 °C and calcined (usually at temperatures of 800–1100 °C).[68,69] This method, including its variations such as self-propagating high-temperature synthesis (instead of prolonged heat treatment, the gel is quickly heated to the temperature required to begin a self-sustaining reaction), and the Pechini method (in this case, cations enter the gel during complexation) is simple to implement but difficult to scale and unsuitable for some systems due to the formation of dense agglomerates of particles in them.[70–72]

The precipitation method involves adding a solution containing metal cations to a precipitant solution (reverse precipitation) or vice versa (direct precipitation). The resulting precipitate contains carbonates, hydroxides, or other metal compounds that can be converted to the oxide form by thermal treatment, i.e., precipitation is a stage preceding solid-phase synthesis. The advantages of the method are its scalability and high chemical homogeneity of the product. At the same time, it requires careful control of the synthesis parameters to ensure the complete precipitation of the elements and the required microstructure. Co-precipitation is widely known as a method for synthesizing powders of the binary crystalline compounds YAG and LuAG garnets,[73–81] as well as for multiatomic gallium–aluminum doped garnets.[82–88]

Co-precipitation differs from the other listed methods in that the required crystalline phase already appears at the stage of preparation of the powdered compound, which has particles with dimensions even in the nanosize domain. This feature allows for a significant reduction in the gallium loss due to evaporation in the form of oxide; gallium is bound in a more complex compound. Figure 5 shows the images obtained by the scanning electron microscopy (SEM) of $(Gd,Y)_3Al_2Ga_3O_{12}$:Ce (GYAGG:Ce) powder obtained at different processing temperatures for 2 h. The method of inverse precipitation allows to synthesize powders with weak agglomeration of particles, which is maintained over a wide temperature range. Weakly agglomerated powders are quickly ground to fractions necessary for obtaining compacts by pressing or 3D printing.[89]

Co-precipitation allows the production of powdered compounds with primary particles of about 50 nm in size and a specific surface area of 60–70 m^2/g. The presence of multiple contacts between the particles provides high sintering capacity, making it possible to obtain dense and transparent ceramics without applying pressure during sintering.

C. Sintering of the ceramics

Optically transparent ceramics may be produced either under the carefully optimized sintering conditions or by the introduction of special sintering additive. The latter make the process easier while may affect scintillation parameters. Sintering conditions include the temperature, time, and atmosphere of high-temperature processing of compacts. Sintering of garnet ceramics requires a temperature of 1600–1800 °C.[86,90–92] For compacts made from co-precipitated powders, the optimal temperature for producing GYAGG transparent ceramics is ∼1700 °C. Figure 6 shows the SEM images of GYAGG:Ce ceramics obtained by sintering at different temperatures.

As seen, the defect-free polycrystalline structure is produced at a sintering temperature of 1700 °C. In addition, with an increase in the sintering temperature, an increase in the average grain size of the ceramics is observed: 0.6 mm at 1500 °C, 1.0 mm at 1600 °C, and 1.4 mm at 1700 °C.

When using particles with a high specific surface area to produce ceramics, a stable correlation between the transparency of the ceramics and the sintering time has not been established, although this dependence has been obtained in binary and ternary compounds.[93,94] This may be due to the high reactivity of the powders obtained by the method of inverse precipitation.

A well-known method to produce transparent ceramics is sintering in a vacuum,[95,96] which is commonly titled "vacuum-tight." However, when sintering gallium-containing compounds in a vacuum, there is a noticeable loss of this component due to its high volatility. Evaporation of gallium from the compact results in nonstoichiometry and leads to a deterioration in the functional properties of the ceramics. An alternative technique is sintering in an oxygen atmosphere.[97–99] Figure 7 shows the samples of various multiatomic garnet ceramics obtained by sintering in an oxygen atmosphere.

Optical transparency is achieved at 2 h of sintering. The bulk porosity is strongly diminished, resulting in low light scattering. An advantage of the sintering in oxygen of the compacts made of high-reactivity powders is clearly seen from Fig. 8. It shows the SEM images of GYAGG:Ce, Tb ceramics obtained by sintering in air and in an oxygen atmosphere. Sintering in oxygen allows to reduce the porosity of the ceramics and increase the average grain size from 0.5 to 1.5 μm. Typical optical transmission of 60% at a wavelength of 520 nm is achieved.

Worth noting, the ceramics samples consist of differently oriented grains, as seen from electron backscatter diffraction (EBSD) maps (Fig. 9). However, the presence of numerous boundaries between crystallites does not lead to a significant decrease in the optical transmittance of the samples.

The utilization of sintering additives also allows improving the transmittance of ceramics by modifying their microstructure. Sintering additives based on silicon and boron[100–102] lead to a significant increase in the average grain size of the ceramics and decrease in the proportion of intergranular boundaries in the bulk of the material. This is due to the formation of a SiO_2 melt (melting point 1600 °C) and a B_2O_3 melt (melting point 480 °C) during the sintering process. An active exchange of components between individual grains of the ceramics is promoted due to the liquid-phase sintering, as seen in Fig. 10. The average grain size of the ceramics with the addition of SiO_2 and B_2O_3 increases from 1.4 to 2.6 and 3.1 μm, respectively.

Under certain conditions, low-melting sintering additives can cause uncontrolled grain growth, worsening the quality of the resulting ceramics. Therefore, in several studies, the SiO_2 additive is introduced together with a grain growth inhibitor, for example, MgO,[103,104] due to the presence of which active grain growth occurs more uniformly. Additives based on ZrO_2 have a positive

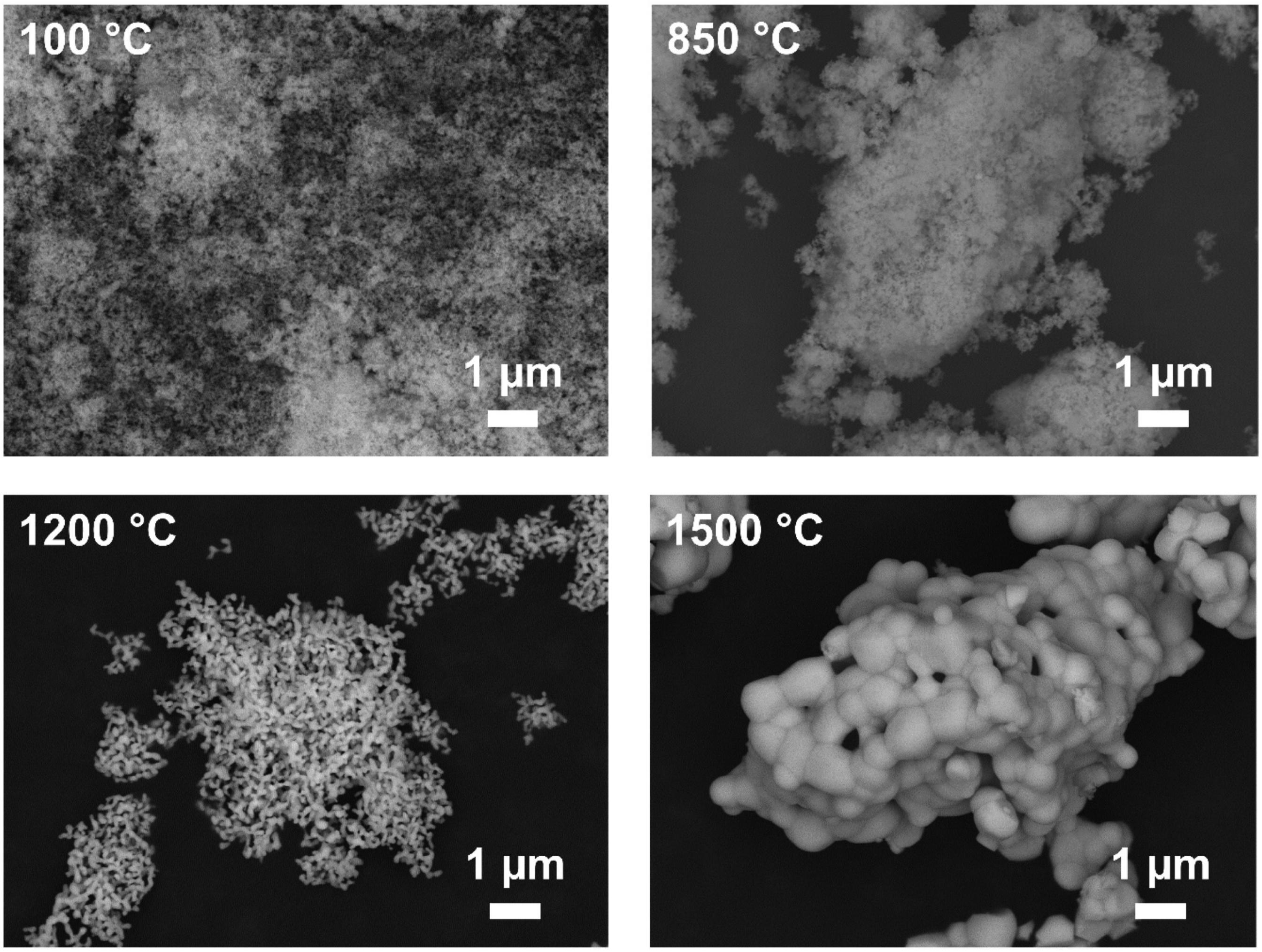

FIG. 5. SEM images of GYAGG:Ce nanopowders calcined at various temperatures.

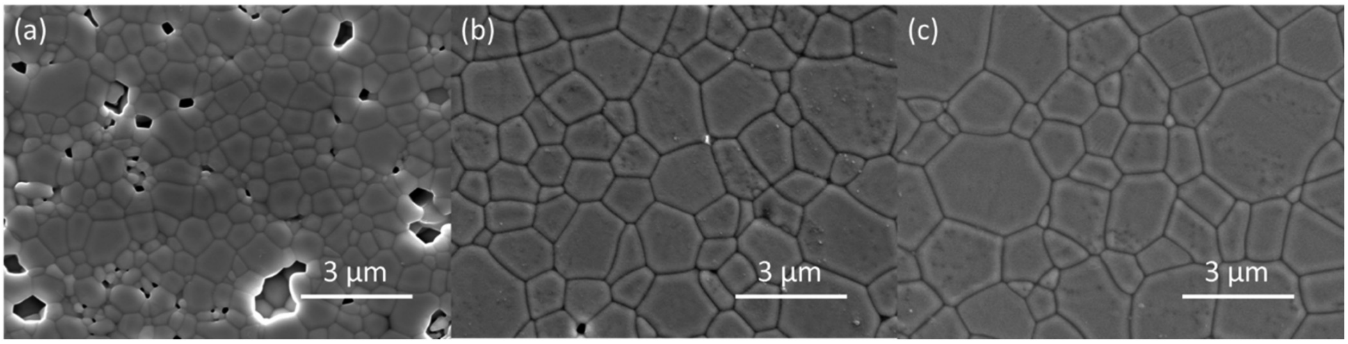

FIG. 6. Scanning electron microscopy images of GYAGG:Ce ceramics obtained by sintering at 1500 (a), 1600 (b), and 1700 °C (c).

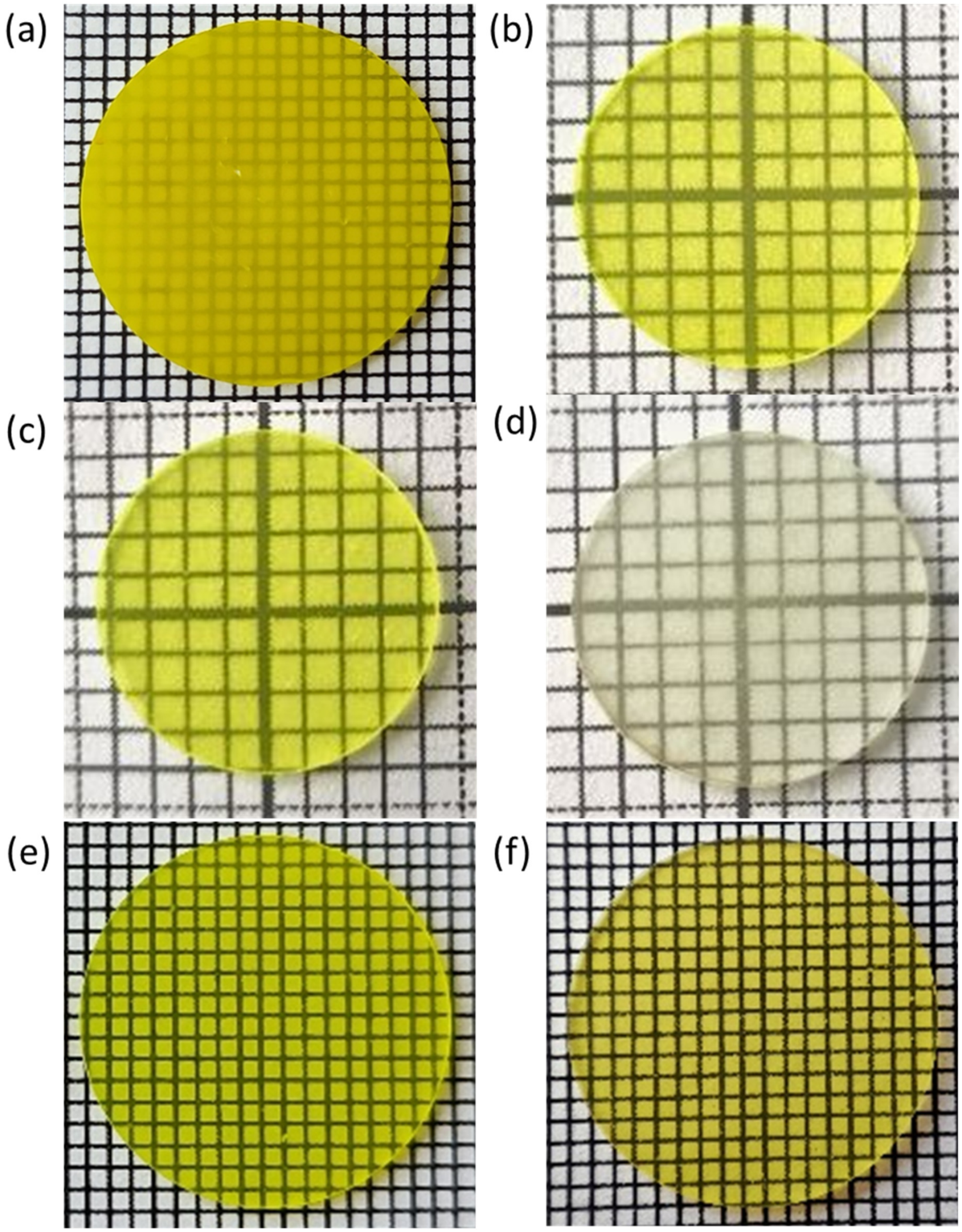

FIG. 7. Transparent ceramics of ternary, quaternary, and quintuple garnets: $Gd_3Al_2Ga_3O_{12}$:Ce (a), $(Gd,\ Y)_3Al_2Ga_3O_{12}$:Ce (b), $(Gd,Y)_3Al_2Ga_3O_{12}$:Ce,Tb (c), $(Gd,Y)_3Al_2Ga_3O_{12}$:Tb (d), $(Gd,Y,Lu)_3Al_2Ga_3O_{12}$:Ce (e), $(Gd,Y)_3Al_2Ga_3O_{12}$:Ce,Yb (f).

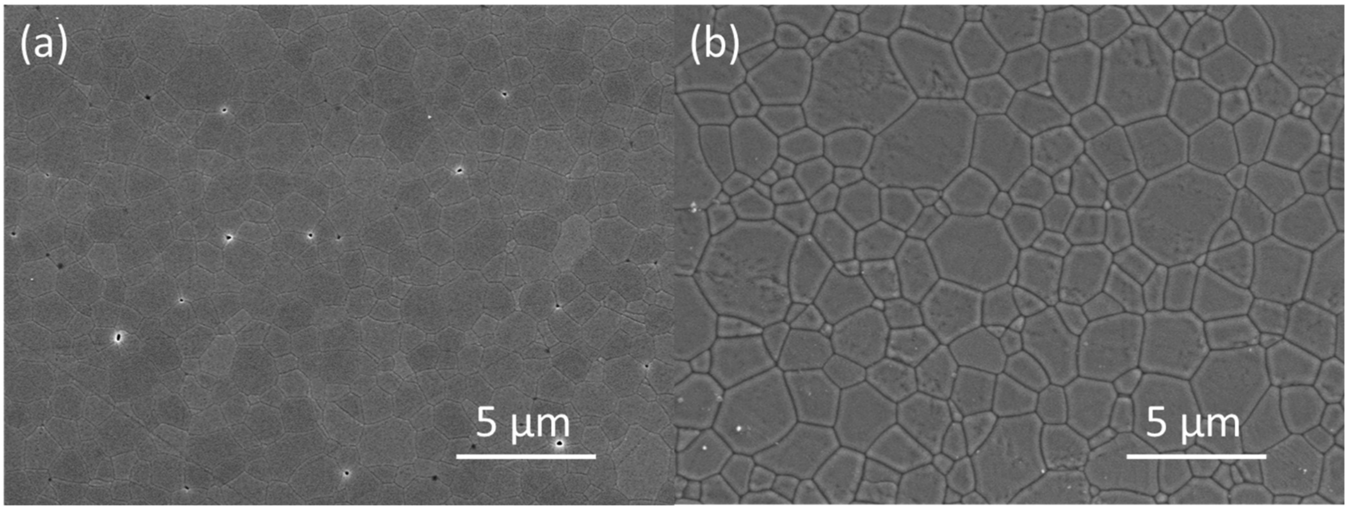

FIG. 8. SEM images of GYAGG:Ce,Tb samples sintered in air (a) and oxygen (b).

effect on the microstructure of garnet-based ceramics[105] as well. Figure 11 shows the SEM images of GYAGG:Ce samples sintered with the additives of MgO and ZrO_2.

The utilization of the sintering additives might be associated with noticeable changes in their luminescence properties. It is known that the addition of MgO allows for a noticeable acceleration of the photoluminescence and scintillation kinetics,[106,107] but it significantly reduces their intensity. For SiO_2 additive, the dependence is not so clear-cut, and with the use of relatively small amounts of the additive, some increase in the scintillation yield was observed.[108,109] The addition of ZrO_2 and B_2O_3 was also studied in Ref. 110: both additives led to an increase in the optical transparency of the material without notable affecting the scintillation light yield and kinetics.

D. Disordered compounds of tungstates with scheelite structure

Recently, encouraging results have been obtained for self-activated scintillators of tungstate compounds made in the powder form, namely, $(Pb,Ca)WO_4$, $(Pb,Sr)WO_4$, and $(Pb,Ba)WO_4$.[43] Due to the disorder in the cationic subsystem by the mixing of Pb–Sr and Pb–Ba ions, the scintillation yield was measured to be significantly high in comparison with the appropriate binary compounds: $PbWO_4$ (PWO), SrWO4, and $BaWO_4$. The above ternary tungstates have a high stopping power for ionizing radiation and can provide the registration of annihilation x rays with good time resolution, which makes them a very attractive option to use in positron emission tomography (PET) scanners in

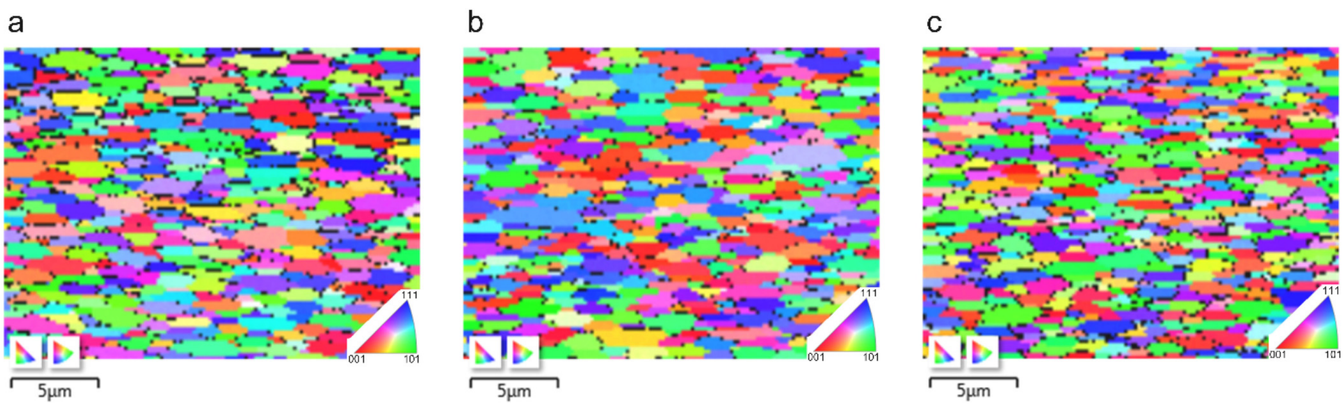

FIG. 9. EBSD maps in grain orientation visualization mode (black pixels are zero solutions) at ×5000 magnification for GYAGG:Tb samples with different Tb contents: (a) x = 0.05, (b) x = 0.10, (c) x = 0.20.

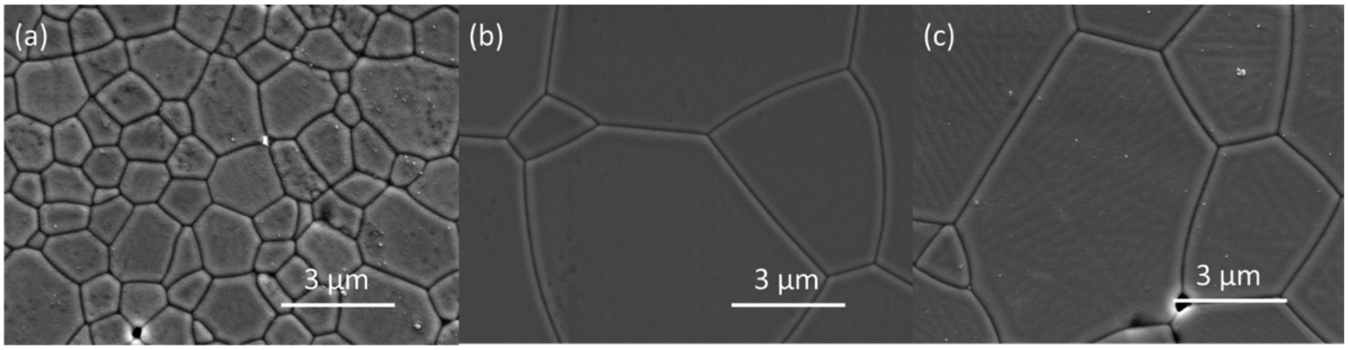

FIG. 10. SEM images of GYAGG:Ce ceramics produced without sintering additives (a), with the addition of 0.01 SiO_2 wt. % (b) and 0.01 wt. % B_2O_3 (c).

the time-of-flight (TOF) registration mode.[111] At the same time, it has been established that $(Pb,Sr)WO_4$ (PSWO) does not form congruently melting compounds.[112] Nevertheless, these materials can be obtained from the melt by crystal growth from the solution in the melt. Figure 12 shows a sample of $(Pb,Sr)WO_4$ grown in the $PbWO_4$ solution.

The scheelite structural type of the mixed single crystals was confirmed by x-ray diffraction measurements. The density of the $(Pb_{0.5}Sr_{0.5})WO_4$ was measured to be 7.39 g/cm^3. The luminescence band in mixed tungstates consists of the three strongly overlapped bands. Figure 13 depicts measured at 150 K photoluminescence spectra of $(Pb_{0.5}Sr_{0.5})WO_4$ $(Pb_{0.5}Sr_{0.5})WO_4$:La and its approximation by three Gaussian-type bands, the temperature dependence of integrated luminescence of these components in undoped and solely doped with La (50 ppm) samples, and samples scintillation kinetics.

As seen, the band peaked in the vicinity of 2.5 eV is affected by La codoping. Most probably, it relates to oxygen vacancies, similarly to PWO, in which WO_3 defect luminescence was strongly suppressed by the La or Y doping.[13] The other bands that contribute to the profile of the luminescence band might correspond to the WO_4^{2-} coupled to the different cations: Sr–WO_4^{2-} or WO_4^{2-}–Pb. A remarkable feature of the luminescence is quite different from PWO, the temperature dependence of the integrated luminescence intensity. All three bands' intensities show the breaking points at the temperature above 250 K. Thus, the luminescence quenching due to the thermoionization of excitons remains a weak process roughly up to the room temperature. This change in the disordered tungstate is crucially important to obtain a high light yield of the self-activated scintillator.

To date, the top results in terms of scintillation parameters have been obtained with single crystals of $(Pb_{0.5}, Sr_{0.5})WO_4$. These

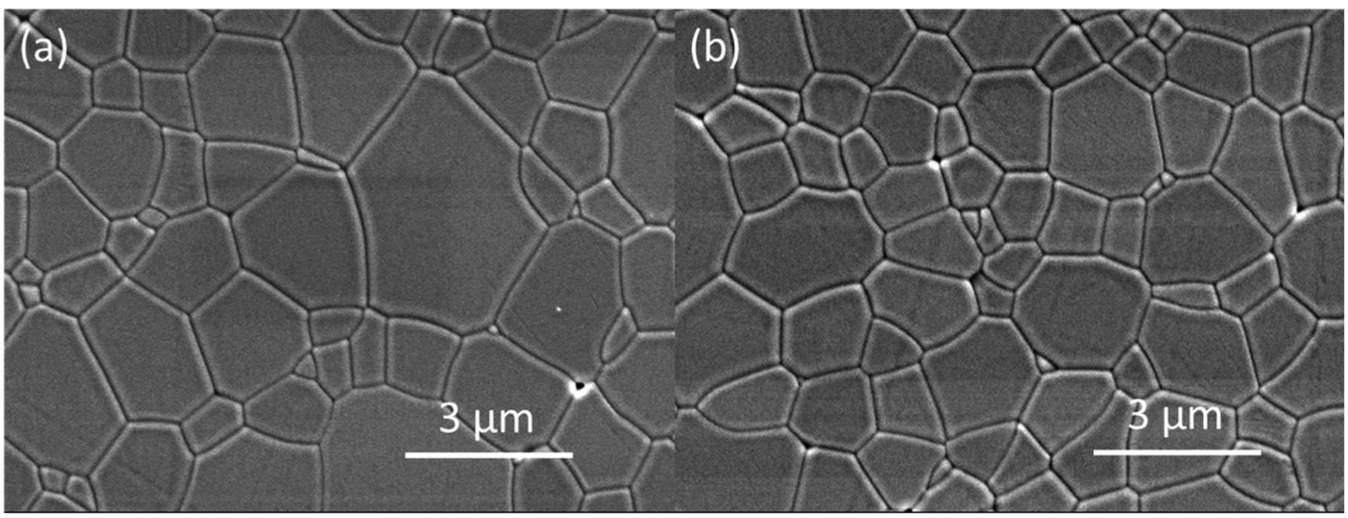

FIG. 11. SEM images of GYAGG:Ce samples produced with the addition of MgO (a) и ZrO_2 (b) in the green bodies.

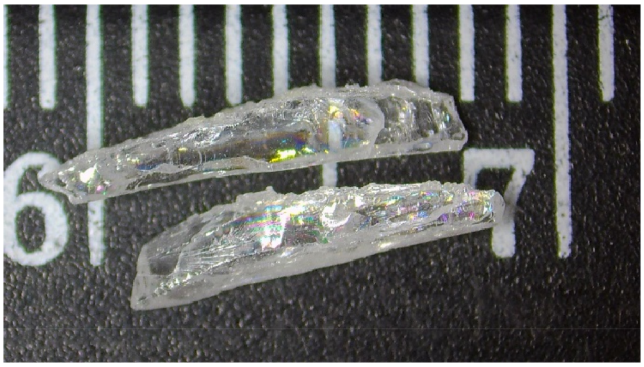

FIG. 12. $(Pb_{0.5}Sr_{0.5})$ WO_4 single crystal produced by the crystallization in the solution of $PbWO_4$.

parameters are given in Table I in comparison with crystals of PWO and $Bi_4Ge_3O_{12}$ (BGO).

E. Disordered phosphates

Compounds of elements of the fifth group, in particular phosphates, are also promising for the creation of scintillation materials along with compounds of ions of the third (Al, Ga) and fourth (Si, Ge) groups of elements.[113–116] Although the scintillation yield in phosphates based on Lu and, apparently, Y does not exceed 20 000 phot/MeV, the compounds are interesting from the point of view of confirming the efficiency of exploiting the disorder in inorganic crystalline scintillators. Since mixing phosphorus and heavier elements of this group in one crystalline system is technologically quite difficult, the preferred option is to create disordered systems by diluting the sublattice of the heavy cation in the compound. The authors[117] established an increase in the integral intensity of luminescence of Eu^{3+} ions upon dilution of the yttrium sublattice with scandium ions in the $Sc_xY_{1-x}PO_4$:Eu^{3+} compound. Recently, the authors[118] have established an almost twofold increase in the quantum yield of intrinsic luminescence in the same crystalline compound at a Sc/Y ratio of about 1 when excited with 10 eV synchrotron radiation. This makes such mixed compounds very promising for increasing the scintillation yield, since yttrium-scandium phosphates form solid solutions with a range of pseudopotential fluctuations as high as 1 eV.

F. Light weight disordered compounds

The commonly exploited idea of scintillators as "heavy" materials was constituted by the use of scintillation crystals for gamma-ray spectrometry, high-energy physics, medical, and security inspection equipment. The high density of the scintillator provides high stopping power for gamma and x-ray radiation and, therefore, allows making the detector module more compact with an acceptable cost. For neutron measurements, high density of materials is more likely to be a disadvantage since higher density causes higher sensitivity to background gamma quanta. Commercially available materials used for neutron detection ^{6}LiI:

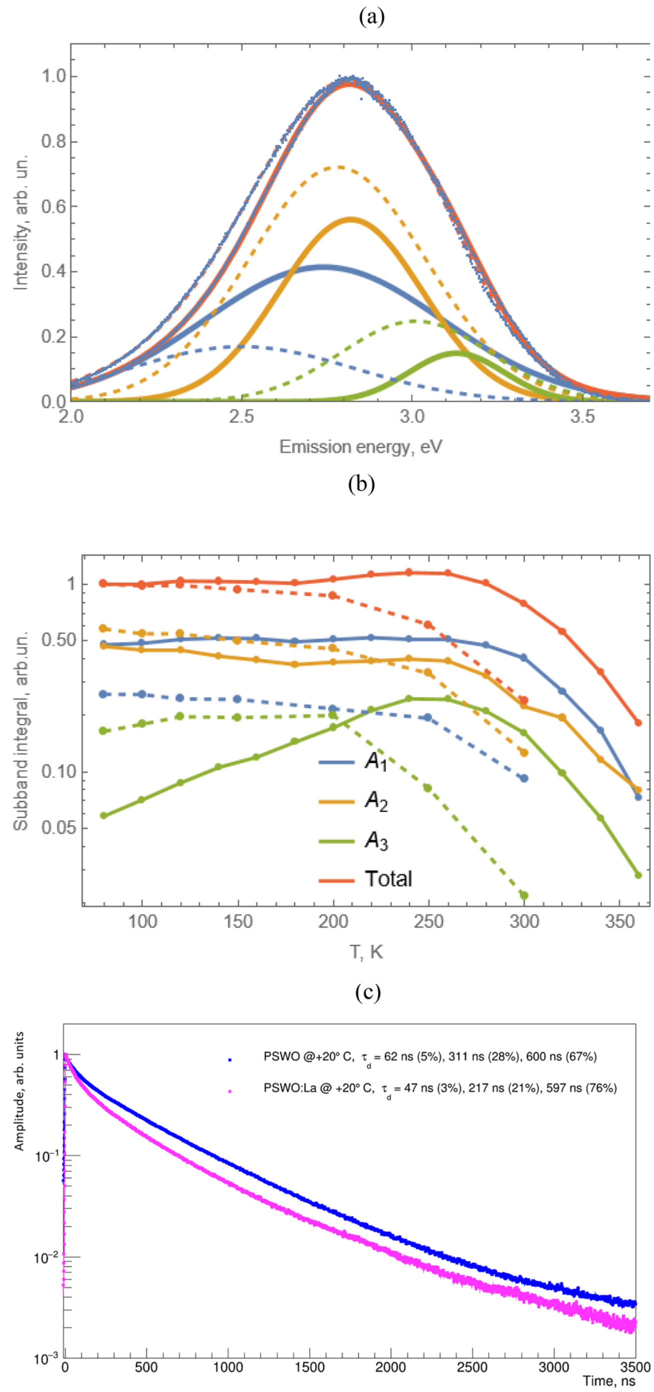

FIG. 13. PSWO (solid) and PSWO:La (dashed) luminescence excited at 280 nm and measured at 150 K and its approximation by three Gaussian-type bands; (a) temperature dependence of the PSWO and PSWO:La luminescence bands integrated intensity in the spectral range 300–650 nm at 280 nm excitation; (b) comparison of room temperature measured scintillation kinetics (c).

TABLE I. Comparison of parameters of PWO, PSWO, and BGO scintillators.

Sample	Density (g/cm^3)	Effective charge (Z_{eff})	Light yield (ph/MeV)	Scintillation band maximum (nm)	Scintillation kinetics components (ns)
PWO	8.28	76	100	420	6
PSWO	7.39	71	13 500	430	500
BGO	7.13	75	8200–9000	505	300

Eu,[119] $Gd_3Al_2Ga_3O_{12}$:Ce,[120] Cs_2LiYCl_6:Ce,[121,122] $CdWO_4$,[123] powdered scintillators ZnS:Ag mixed with neutron converter ^{6}LiF,[124] and Gd^2O_2S:Tb[125] have a relatively high stopping power for gamma-radiation. In this context, lightweight inorganic scintillation materials combining light cations and anions and allowing isovalent doping with rare earth ions are of interest. Lanthanum chloride $LaCl_3$:Ce[126] meets this criterion and has proven itself well for detecting fast neutrons. Table II summarizes some properties of relatively light inorganic compounds that satisfy the selection criterion.

$$^{*}Z_{\text{eff}} = \sqrt[n]{\sum_i \omega_i Z_i^n},$$

where ω is the mass fraction of an element with atomic number Z_i, $n = 4$.[127]

First, consider $LiAlO_2$ having the lowest effective charge of the compound. In tetragonal $LiAlO_2$, aluminum atoms have tetrahedral coordination with oxygen atoms. This type of coordination is not suitable for the localization of rare earth ions. However, the $LiAlO_2$ compound exists in three possible allotropic forms: low-temperature $LiAlO_2$ (up to 400 °C); intermediate $LiAlO_2$ (400–800 °C); and $LiAlO_2$, stable at high temperatures (>1000 °C). Perhaps, it is possible to introduce RE ions into the rhombohedral $LiAlO_2$, in which aluminum atoms have octahedral coordination. However, since this compound is actually intermediate and does not exist at low temperatures, no successful attempts to introduce a rare earth ion into the $LiAlO_2$ matrix have been observed. Self-activated scintillators based on $LiAlO_2$ have a low light yield for neutron detection, amounting to 7000 ph/neutron. When doped with copper, the light yield can be increased to 9000 ph/neutron.[128] Obviously, the use of fluorides does not have much promise because fluoride-based materials have a wide bandgap and, as a consequence, a reduced scintillation yield.[13] li_3YCl_6 is a very attractive compound, but it is also considered a promising solid-state electrolyte.[128] From the point of view of the combination of low density and high light yield of scintillations, nitrides $LiCaAlN_2$ and $LiCaAl_3N_4$ are of interest: their bandgap is less than 3 eV, and the effective charge is 16.3 and 14.8, respectively. These matrices have shown excellent characteristics as phosphors.[129]

TABLE II. Lightweight inorganic materials that are promising for creating scintillators for neutron detection.

Compound	Density (g/cm^3)	Eg (eV)	Concentration of atoms interacting with neutrons (cm^{-3})	Z_{eff}*
LiI:Eu	4.08	4.23	1.83×10^{22}	52.3
$LaCl_3$	3.8	3.65	2.69×10^{22}	49.5
$CeCl_3$	3.9	4.3	2.86×10^{22}	50.4
$LiYO_2$	4.1	4.01	1.93×10^{22}	35.6
$LiYSiO_4$	3.65	5.11	1.17×10^{22}	32.4
Li_3YCl_6	2.45	6.47	1.37×10^{22} li 2.74×10^{22} Cl	28.9
$LiGdCl_4$	3.7	0.91	7.28×10^{21} li 7.27×10^{21} Gd 2.91×10^{22} Cl	54.2
γ-$LiAlO_2$	2.64	4.59	2.4×10^{22}	11.0
$LiCaAlF_6$	2.86	7.64	9.15×10^{21}	14.3
Li_2MgSiO_4	2.48	4.94	2.29×10^{22}	13.2
Li_2CaSiO_4	2.86	5.19	2.35×10^{22}	16.2
Li_2SrSiO_4	3.43	4.64	2.13×10^{22}	31.3
Li_2BaSiO_4	3.88	4.39	2.17×10^{22}	48.6
$LiCaAlN_2$	2.91	2.78	1.72×10^{22}	16.3
$LiCaAl_3N_4$	2.99	3.02	9.78×10^{21}	14.8

Next in density from the above listed set of the materials are silicates. The scintillation properties of these materials when activated by Eu^{2+} ions have been confirmed by the authors.[130,131] The group of compounds Li_2AESiO_4, where AE = Mg, Ca, Sr, and Ba, is of particular interest. One of the advantages of this group is the possibility of growing a single-crystal material.[132] Increasing the light yield of Li_2CaSiO_4 seems possible by creating compositional disorder. Note that in the series of Li_2AESiO_4 compounds, Li_2CaSiO_4 has the widest bandgap, so the dilution of the Ca^{2+} sublattice with Mg^{2+}, Sr^{2+}, and Ba^{2+} ions seems promising. Of course, with an increase in the number of ions "heavier" than calcium, the effective charge of the compound will also increase.

An expected issue in the creation of compositionally disordered lightweight silicates is the mutual solubility of ions in the matrix. In the series $Li_2MgSiO_4 \rightarrow Li_2CaSiO_4 \rightarrow Li_2SrSiO_4 \rightarrow Li_2BaSiO_4$, the crystal structure changes with modification in the symmetry of the lattice of the compounds: Li_2MgSiO_4 is monoclinic, Li_2CaSiO_4 is tetragonal, Li_2SrSiO_4 is trigonal, and Li_2BaSiO^4 is hexagonal. All this indicates that the mutual solubility of the AE ions (Ca^{2+}, Mg^{2+}, Sr^{2+}, and Ba^{2+}) in the Li_2AESiO_4 matrix is limited, unlike cubic matrices with a garnet structure, in which oxides similar in chemical properties and structure dissolve in each other almost unlimitedly.[133] At the same time, the spectroscopic parameters in mixed compounds are quite difficult to predict. Figures 14(a) and 14(b) show the luminescence and its excitation spectra measured at room temperature in the compounds Li_2CaSiO_4, $Li_2Sr_{0.1}Ca_{0.9}$SiO4, and Li_2SrSiO_4 activated by Eu^{2+} ions. At a small fraction of Ca ions, which were substituted by Sr ions, luminescence spectra do not show many

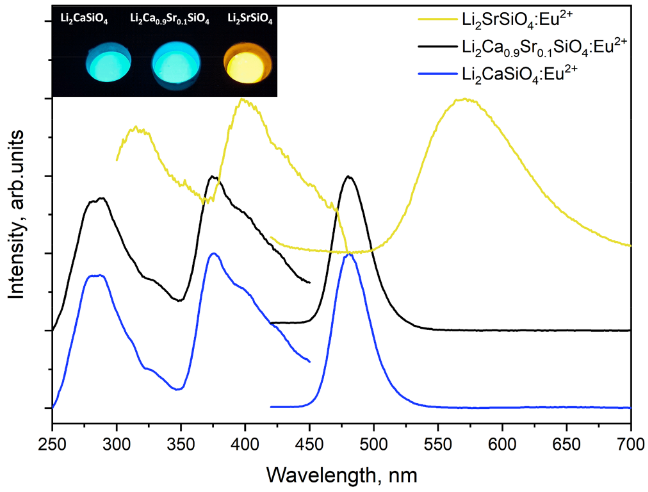

FIG. 14. The luminescence and luminescence excitation spectra measured at room temperature in the activated by Eu^{2+} ions compounds Li_2CaSiO_4, $Li_2Sr_{0.1}Ca_{0.9}SiO_4$, and Li_2SrSiO_4.

changes, whereas a strong red shift of the luminescence is observed in the Ca free compound.

This gives hope that the introduction of disorder into the cation sublattice in the lightweight compounds gives a spare for manipulation and future improvement of scintillation properties, as has been established for compounds of the garnet structural type.

IV. PORSPECTS OF THE METHOD

A question that requires further investigation is the confirmation of the universality of the method for all types of scintillation materials, including cross-luminescent species. Until now, non-isovalent doping has been intensively studied in these materials, and only recently, the results have appeared on BaFCl activated by Eu^{2+} with a scintillation yield of more than 10 000 photons/MeV.[134,135] The yield of the cross-luminescence in an undoped mixed material under excitation by ionizing radiation has not been analyzed. It can only be assumed that the modulation of the bottom and top of the valence band in the material would lead to some spectral shift of cross-luminescence, but it is difficult to judge the change in the scintillation yield. At the same time, the available experimental data on activated and now self-activated scintillators show that careful optimization of the technological aspects of the multicationic material production promotes successful progress in improving their scintillation properties. The fact that most of the results in the area of interest were obtained for Al–Ga garnets indicates the greatest technological development of compounds of this structural class. Among the technologies to produce garnets, we note the promise of the ceramic method for obtaining the material, while the single-phase contamination, transmittance, and preservation of the concentration of activators in the required valence state are ensured by both the chosen method for obtaining precursors and the sintering conditions. The developed technological chain can be supplemented and improved, but it should be understood that the listed properties must be ensured. So far, there are no visible limitations on increasing the amount of RE ions in the matrix while maintaining substitution isomorphism. However, an obvious limitation is the need to maintain the integrity of the system for excitation transfer along the cationic RE ions subsystem. Gd^{3+} ions cope well with this role in many matrices; however, the dilution of its sublattice has a lower limit. The combination of RE ions and yttrium in the lattice is more aimed at changing the stopping power of the matrix for ionizing radiation or at adjusting the resonance conditions of excitation transfer. In garnets, formed by 3^+ cations, the major contribution to the modulation of the conduction band bottom is made by the random distribution of Al and Ga ions localized in tetrahedra and octahedra. From this point of view, silicate garnets, i.e., garnets based on 2^+ and 4^+ cations, abundant in nature, are of certain interest. One of the advantages of such materials is a smaller forbidden zone, which can act as an additional factor in increasing the scintillation yield.

V. CONCLUSIONS

This review summarizes the evidence of the compositional disordering of the crystalline matrices of the oxide scintillation materials, activated and self-activated, to improve their scintillation parameters. A few effects of the compositional disorder in the crystalline system have been highlighted. First is a change in the landscape of the top and bottom regions of the valence and conduction bands, which are adjacent to the bandgap. Second, managing the modulation of bandgap at the subnanoscale level promotes the efficient energy loss by carriers during thermalization, their smaller spatial dispersion, and, consequently, more efficient binding into excitons and, further, an increase in the scintillation yield.

This approach was generalized for activated and self-activated inorganic scintillators and supported by the results on the luminescence and the scintillation properties improvement obtained with scintillation crystalline compounds of the garnet and scheelite structural types. It is shown that this way of engineering the compound's composition may result in an increase in the yield of scintillation, a shortening in the kinetics of scintillation, or a combination of both. This is due to the increasing role of geminate pairs of nonequilibrium carriers in the transfer of electronic excitations to luminescent centers, as well as the increasing role of exchange interaction, which reduces the role of long-range electronic excitation transport, in particular, in Gd^{3+}-based crystals. The results on the scintillation properties of the complication of the crystal composition—from binary to quintuple cation garnet type ceramic compounds, containing Gd, Y, Lu, Tb, and Yb matrix-forming ions—and from binary to ternary tungstate crystals are discussed in support of the developed approach.

ACKNOWLEDGMENTS

The authors acknowledge the support from the Russian Ministry of Science and Education, Agreement No. 075-15-2021-1353 dated 10.12.2021. Analytical research was done using equipment of Research Chemical and Analytical Center NRC Kurchatov Institute Shared Research Facilities. The authors at

Belarus State University acknowledge the Belarusian Republican Foundation for Fundamental Research, Grant No. F23-RSF-074.

AUTHOR DECLARATIONS

Conflict of Interest

The authors have no conflicts to disclose.

Author Contributions

M. Korzhik: Conceptualization (equal); Writing – original draft (equal). **V. Retivov:** Conceptualization (equal). **V. Dubov:** Investigation (equal). **V. Ivanov:** Writing – original draft (equal). **I. Komendo:** Writing – original draft (equal). **D. Lelekova:** Writing – review & editing (equal). **P. Karpyuk:** Investigation (equal). **V. Mechinsky:** Investigation (equal). **A. Postupaeva:** Formal analysis (equal). **V. Smyslova:** Methodology (equal). **V. Shlegel:** Formal analysis (equal). **I. Shpinkov:** Investigation (equal). **A. Vasil'ev:** Writing – review & editing (equal).

DATA AVAILABILITY

The data that support the findings of this study are available within the article.

REFERENCES

[1]R.-Z. Zhang and M. J. Reece, "Review of high entropy ceramics: Design, synthesis, structure and properties," J. Mater. Chem. A **7**(39), 22148–22162 (2019).

[2]J. Perego, C. X. Bezuidenhout, I. Villa, F. Cova, R. Crapanzano, I. Frank, F. Pagano, N. Kratochwill, E. Auffray, S. Bracco, A. Vedda, C. Dujardin, P. E. Sozzani, F. Meinardi, A. Comotti, and A. Monguzzi, "Highly luminescent scintillating hetero-ligand MOF nanocrystals with engineered Stokes shift for photonic applications," Nat. Commun. **13**(1), 3504 (2022).

[3]M. A. K. Sheikh, D. Kowal, M. H. Mahyuddin, D. Onggo, F. Maddalena, C. Dang, R. Cala', E. Auffray, M. E. Witkowski, M. Makowski, W. Drozdowski, D. Cortecchia, C. Dujardin, and M. D. Birowosuto, "Solution-Processable A_2XY_4 (A = PEA, BA; X = Pb, Sn, Cu, Mn; Y = Cl, Br, I) crystals for high light yield and ultrafast scintillators," IEEE Trans. Nucl. Sci. **70**(7), 1384–1391 (2023).

[4]O. Sidletskiy, V. Gorbenko, T. Zorenko, Y. Syrotych, S. Witkiwicz-Łukaszek, J. A. Mares, R. Kucerkova, M. Nikl, I. Gerasymov, D. Kurtsev, A. Fedorov, and Y. Zorenko, "Composition engineering of $(Lu,Gd,Tb)_3(Al,Ga)_5O_{12}$:Ce film/$Gd_3(Al,Ga)_5O_{12}$:Ce substrate scintillators," Crystals **12**(10), 1366 (2022).

[5]W. Shao and J. Kim, "Metal-free organic phosphors toward fast and efficient room-temperature phosphorescence," Acc. Chem. Res. **55**(11), 1573–1585 (2022).

[6]M. Irie, T. Fukaminato, T. Sasaki, N. Tamai, and T. Kawai, "A digital fluorescent molecular photoswitch," Nature **420**(6917), 759–760 (2002).

[7]D. A. Sherman, W. Kamal, S. J. Elston, A. A. Castrejón-Pita, S. M. Morris, and J.-C. Tan, "Stable photoinduced metal-organic nanosheet blue phosphor for white light emission," Mater. Today Chem. **38**, 102089 (2024).

[8]O. B. Petrova, K. I. Runina, M. N. Mayakova, I. V. Taydakov, A. V. Khomyakov, R. I. Avetisov, and I. C. Avetissov, "Luminescent hybrid materials based on metal-organic phosphors in PbF_2 powder and PbF_2-containing glass matrix," Opt. Mater. **88**, 378–384 (2019).

[9]G. Huber, C. Kränkel, and K. Petermann, "Solid-state lasers: Status and future [invited]," J. Opt. Soc. Am. B **27**(11), B93–B105 (2010).

[10]N. Zheludev, "The life and times of the LED—A 100-year history," Nat. Photonics **1**(4), 189–192 (2007).

[11]V. Bachmann, C. Ronda, and A. Meijerink, "Temperature quenching of yellow Ce^{3+} luminescence in YAG:Ce," Chem. Mater. **21**(10), 2077–2084 (2009).

[12]M. H. Crawford, "LEDs for solid-state lighting: Performance challenges and recent advances," IEEE J. Sel. Top. Quantum Electron. **15**(4), 1028–1040 (2009).

[13]P. Lecoq, A. Gektin, and M. Korzhik, *Inorganic Scintillators for Detector Systems* (Springer International Publishing, Cham, 2017). ISBN 978-3-319-45521-1.

[14]G. Blasse and A. Bril, "A new phosphor for flying-spot cathode-ray tubes for color television: Yellow-emitting $Y_3Al_5O_{12}:Ce^{3+}$," Appl. Phys. Lett. **11**(2), 53–55 (1967).

[15]R. Autrata, P. Schauer, J. Kuapil, and J. Kuapil, "A single crystal of YAG-new fast scintillator in SEM," J. Phys. E: Sci. Instrum. **11**(7), 707–708 (1978).

[16]C. L. Melcher and J. S. Schweitzer, "Cerium-doped lutetium oxyorthosilicate: A fast, efficient new scintillator," IEEE Trans. Nucl. Sci. **39**(4), 502–505 (1992).

[17]B. H. T. Chai, D. Y. Chai, and R. A. Lux, U.S. patent 7397034B2 (8 July 2008).

[18]M. Korjik, A. Bondarau, G. Dosovitskiy, V. Dubov, K. Gordienko, P. Karpuk, I. Komendo, D. Kuznetsova, V. Mechinsky, V. Pustovarov, V. Smyslova, D. Tavrunov, and V. Retivov, "Lanthanoid-doped quaternary garnets as phosphors for high brightness cathodoluminescence-based light sources," Heliyon **8**(8), e10193 (2022).

[19]M. Korzhik, R. Abashev, A. Fedorov, G. Dosovitskiy, E. Gordienko, I. Kamenskikh, D. Kazlou, D. Kuznecova, V. Mechinsky, V. Pustovarov, V. Retivov, and A. Vasil'ev, "Towards effective indirect radioisotope energy converters with bright and radiation hard scintillators of $(Gd,Y)_3Al_2Ga_3O_{12}$ family," Nucl. Eng. Technol. **54**(7), 2579–2585 (2022).

[20]P. Karpyuk, M. Korzhik, A. Fedorov, I. Kamenskikh, I. Komendo, D. Kuznetsova, E. Leksina, V. Mechinsky, V. Pustovarov, V. Smyslova, V. M. Retivov, Y. Talochka, D. Tavrunov, and A. Vasil'ev, "The saturation of the response to an electron beam of Ce- and Tb-doped GYAGG phosphors for indirect β-voltaics," Appl. Sci. **13**(5), 3323 (2023).

[21]M. Korjik and E. Auffray, "Limits of inorganic scintillating materials to operate in a high dose rate environment at future collider experiments," IEEE Trans. Nucl. Sci. **63**(2), 552–563 (2016).

[22]A. Barysevich, V. Dormenev, A. Fedorov, M. Glaser, M. Kobayashi, M. Korjik, F. Maas, V. Mechinski, R. Rusack, A. Singovski, and R. Zoueyski, "Radiation damage of heavy crystalline detector materials by 24 GeV protons," Nucl. Instrum. Methods Phys. Res., Sect. A **701**, 231–234 (2013).

[23]E. Auffray, A. Fedorov, M. Korjik, M. Lucchini, V. Mechinski, N. Naumenko, and A. Voitovich, "Radiation damage of oxy-orthosilicate scintillation crystals under gamma and high energy proton irradiation," IEEE Trans. Nucl. Sci. **61**(1), 495–500 (2014).

[24]E. Auffray, A. Borisevitch, A. Gektin, I. Gerasymov, M. Korjik, D. Kozlov, D. Kurtsev, V. Mechinsky, O. Sidletskiy, and R. Zoueyski, "Radiation damage effects in Y_2SiO_5:Ce scintillation crystals under γ-quanta and 24 GeV protons," Nucl. Instrum. Methods Phys. Res., Sect. A **783**, 117–120 (2015).

[25]E. Auffray, A. Fedorov, V. Dormenev, J. Houžvička, M. Korjik, M. T. Lucchini, V. Mechinsky, and S. Ochesanu, "Optical transmission damage of undoped and Ce doped $Y_3Al_5O_{12}$ scintillation crystals under 24 GeV protons high fluence," Nucl. Instrum. Methods Phys. Res., Sect. A **856**, 7–10 (2017).

[26]E. Auffray, A. Barysevich, A. Fedorov, M. Korjik, M. Koschan, M. Lucchini, V. Mechinski, C. L. Melcher, and A. Voitovich, "Radiation damage of LSO crystals under γ- and 24 GeV protons irradiation," Nucl. Instrum. Methods Phys. Res., Sect. A **721**, 76–82 (2013).

[27]E. Auffray, G. Dosovitskiy, A. Fedorov, I. Guz, M. Korjik, N. Kratochwill, M. Lucchini, S. Nargelas, D. Kozlov, V. Mechinsky, P. Orsich, O. Sidletskiy, G. Tamulaitis, and A. Vaitkevičius, "Irradiation effects on $Gd_3Al_2Ga_3O_{12}$ scintillators prospective for application in harsh irradiation environments," Radiat. Phys. Chem. **164**, 108365 (2019).

[28]V. Alenkov, O. Buzanov, G. Dosovitskiy, V. Egorychev, A. Fedorov, A. Golutvin, Y. Guz, R. Jacobsson, M. Korjik, D. Kozlov, V. Mechinsky, A. Schopper, A. Semennikov, P. Shatalov, and E. Shmanin, "Irradiation studies of a multi-doped $Gd_3Al_2Ga_3O_{12}$ scintillator," Nucl. Instrum. Methods Phys. Res., Sect. A **916**, 226–229 (2019).

[29]V. Retivov, V. Dubov, I. Komendo, P. Karpyuk, D. Kuznetsova, P. Sokolov, Y. Talochka, and M. Korzhik, "Compositionally disordered crystalline

compounds for next generation of radiation detectors," Nanomaterials **12**(23), 4295 (2022).
[30]D. Zhu, M. Nikl, W. Chewpraditkul, and J. Li, "Development and prospects of garnet ceramic scintillators: A review," J. Adv. Ceram. **11**(12), 1825–1848 (2022).
[31]Y. Talochka, A. Vasil'ev, M. Korzhik, and G. Tamulaitis, "Impact of compositional disorder on electron migration in lutetium–yttrium oxyorthosilicate scintillator," J. Appl. Phys. **132**(5), 053101 (2022).
[32]L. Martinazzoli, S. Nargelas, P. Boháček, R. Calá, M. Dušek, J. Rohlíček, G. Tamulaitis, E. Auffray, and M. Nikl, "Compositional engineering of multicomponent garnet scintillators: Towards an ultra-accelerated scintillation response," Mater. Adv. **3**(17), 6842–6852 (2022).
[33]S. Nargelas, A. Solovjovas, Y. Talochka, Ž Podlipskas, M. Kucera, Z. Lucenicova, and G. Tamulaitis, "Influence of heavy magnesium codoping on emission decay in Ce-doped multicomponent garnet scintillators," J. Mater. Chem. C **11**(35), 12007–12015 (2023).
[34]V. Retivov, V. Dubov, D. Kuznetsova, A. Ismagulov, and M. Korzhik, "Gd^{3+} content optimization for mastering high light yield and fast $Gd_xAl_2Ga_3O_{12}:Ce^{3+}$ scintillation ceramics," J. Rare Earths **41**(12), 1911–1918 (2023).
[35]M. Korzhik, V. Retivov, G. Dosovitskiy, V. Dubov, I. Kamenskikh, P. Karpuk, I. Komendo, D. Kuznetsova, V. Smyslova, V. Mechinsky, and A. Vasil'ev, "First observation of the scintillation cascade in Tb^{3+} -doped quaternary garnet ceramics," Phys. Status Solidi RRL **17**(4), 2200368 (2023).
[36]M. Korzhik, V. Retivov, A. Bondarau, G. Dosovitskiy, V. Dubov, I. Kamenskikh, P. Karpuk, D. Kuznetsova, V. Smyslova, V. Mechinsky, V. Pustovarov, D. Tavrunov, E. Tishchenko, and A. Vasil'ev, "Role of the dilution of the Gd sublattice in forming the scintillation properties of quaternary $(Gd, Lu)_3Al_2Ga_3O_{12}$: Ce ceramics," Crystals **12**(9), 1196 (2022).
[37]K. Omuro, M. Yoshino, K. Bartosiewicz, T. Horiai, R. Murakami, K. J. Kim, K. Kamada, R. Kucerkova, V. Babin, M. Nikl, A. Yamaji, T. Hanada, Y. Yokota, S. Kurosawa, Y. Ohashi, H. Sato, and A. Yoshikawa, "Insights into luminescence and energy transfer processes in Ce^{3+}- and Tb^{3+} co-doped $(Gd, Y)_3Al_2Ga_3O_{12}$ garnet single crystals," J. Lumin. **273**, 120663 (2024).
[38]Z. J. Corey, P. Lu, G. Zhang, Y. Sharma, B. X. Rutherford, S. Dhole, P. Roy, Z. Wang, Y. Wu, H. Wang, A. Chen, and Q. Jia, "Structural and optical properties of high entropy $(La, Lu, Y, Gd, Ce)AlO_3$ perovskite thin films," Adv. Sci. **9**(29), 2202671 (2022).
[39]G. Zhang and Y. Wu, "High-entropy transparent ceramics: Review of potential candidates and recently studied cases," Int. J. Appl. Ceram. Technol. **19**(2), 644–672 (2022).
[40]C. Dujardin, A. Garcia-Murillo, C. Pedrini, C. Madej, C. Goutaudier, A. Koch, A. G. Petrosyan, and M. J. Weber, "Synthesis and scintillation properties of some dense x-ray phosphors," in *Proceedings of International Conference on Inorganic Scintillators and Their Applications (SCINT99), Moscow, Russia, August 1999*, edited by V. Mikhaillin (2000), pp. 527–531. arXiv:2305.08485 [cond-mat.mtrl-sci] (2023).
[41]K. Sreebunpeng, W. Chewpraditkul, W. Chewpraditkul, R. Kucerkova, A. Beitlerova, M. Nikl, T. Szczesniak, M. Grodzicka-Kobylka, D. Zhu, C. Hu, and J. Li, "Luminescence and scintillation properties of fast Ce, $Mg:Lu_2YGa_xAl_{5-x}O_{12}$ ceramic scintillators fabricated from co-precipitated powders," Opt. Mater. **152**, 115418 (2024).
[42]W. Chewpraditkul, T. Horiai, A. Beitlerova, R. Kucerkova, V. Babin, A. Yoshikawa, W. Chewpraditkul, and M. Nikl, "Temperature dependence of photo- and radio-luminescence and scintillation properties of $Lu_2YAl_{2.5}Ga_{2.5}O_{12}$: Ce, Mg multicomponent garnet crystals," Opt. Mater. **147**, 114738 (2024).
[43]M. Korzhik, D. Blau, A. Fedorov, A. Bondarau, Y. Borovlev, A. Amelina, I. Komendo, D. Kuznetsova, A. Mikhlin, V. Mechinsky, A. Postupaeva, V. Shlegel, Y. Talochka, and V. Uglov, "Compositionally disordered tungstate scintillation materials," Radiat. Meas. **167**, 106987 (2023).
[44]A. V. Gektin, A. N. Belsky, and A. N. Vasil'ev, "Scintillation efficiency improvement by mixed crystal use," IEEE Trans. Nucl. Sci. **61**(1), 262–270 (2014).
[45]M. Korzhik, G. Tamulaitis, and A. N. Vasil'ev, *Physics of Fast Processes in Scintillators* (Springer, Cham, 2020). ISBN 978-3-030-21965-9.
[46]J. B. Birks, *The Theory and Practice of Scintillation Counting: International Series of Monographs in Electronics and Instrumentation* (Elsevier, 2013). ISBN 978-1-4831-5606-4.
[47]W. W. Wolszczak and P. Dorenbos, "Non-proportional response of scintillators to alpha particle excitation," IEEE Trans. Nucl. Sci. **64**(6), 1580–1591 (2017).
[48]A. Belsky, F. Gektin, and A. Vasil'ev, "Influence of disorder in scintillating solid solutions on thermalization and recombination of electronic excitations," Phys. Status Solidi B **257**, 1900535 (2020).
[49]See https://materialsproject.org/materials for "Materials project—Materials explorer" (accessed June 4, 2024).
[50]See https://yauhenitalochkan.github.io/CMAP_Docs/ for "CMAP (Condensed Matter And Particles)" (accessed December 31, 2024).
[51]M. Korzhik, V. Alenkov, O. Buzanov *et al.*, "Nanoengineered $Gd_3Al_2Ga_3O_{12}$ scintillation materials with disordered garnet structure for novel detectors of ionizing radiation," Cryst. Res. Technol. **54**, 1800172 (2019).
[52]E. Auffray, R. Augulis, A. Fedorov, G. Dosovitskiy, L. Grigorjeva, V. Gulbinas, M. Koschan, M. Lucchini, C. Melcher, S. Nargelas, G. Tamulaitis, A. Vaitkevičius, A. Zolotarjovs, and M. Korzhik, "Excitation transfer engineering in Ce-doped oxide crystalline scintillators by codoping with alkali-earth ions," Phys. Status Solidi A **215**(7), 1700798 (2018).
[53]G. Tamulaitis *et al.*, "Improvement of the time resolution of radiation detectors based on $Gd_3Al_2Ga_3O_{12}$ scintillators with SiPM readout," IEEE Trans. Nucl. Sci. **66**(7), 1879–1888 (2019).
[54]V. Babin, P. Bohacek, A. Krasnikov, M. Nikl, L. Vasylechko, and S. Zazubovich, "Photoluminescence optical and thermal quenching in heavily doped $Gd_3(Ga,Al)_5O_{12}$:Ce, Mg single crystals: Dependence on the Ga^{3+}, Ce^{3+}, and Mg^{2+} concentration," J. Lumin. **277**, 120945 (2025).
[55]M. Korzhik, V. Alenkov, O. Buzanov, G. Dosovitskiy, A. Fedorov, D. Kozlov, V. Mechinsky, S. Nargelas, G. Tamulaitis, and A. Vaitkevičius, "Engineering of a new single-crystal multi-ionic fast and high-light-yield scintillation material $(Gd_{0.5}–Y_{0.5})_3Al_2Ga_3O_{12}$:Ce, Mg," CrystEngComm **22**(14), 2502–2506 (2020).
[56]K. Kamada, S. Kurosawa, P. Prusa, M. Nikl, V. Kochurikhin, T. Endo, K. Tsutumi, H. Sato, Y. Yokota, K. Sugiyama, and A. Yoshikawa, "Cz grown 2-in. size Ce: $Gd_3(Al, Ga)_5O_{12}$ single crystal; relationship between Al, Ga site occupancy and scintillation properties," Opt. Mater. **36**, 1942–1945 (2014).
[57]M. Korjik, K.-T. Brinkmann, G. Dosovitskiy, V. Dormenev, A. Fedorov, D. Kozlov, V. Mechinsky, and H.-G. Zaunick, "Compact and effective detector of the fast neutrons on a base of Ce-doped $Gd_3Al_2Ga_3O_{12}$ scintillation crystal," IEEE Trans. Nucl. Sci. **66**(1), 536–540 (2019).
[58]I. Gerasymov, T. Nepokupnaya, A. Boyarintsev, O. Sidletskiy, D. Kurtsev, O. Voloshyna, O. Trubaieva, Y. Boyarintseva, T. Sibilieva, A. Shaposhnyk, O. Opolonin, and S. Tretyak, "GAGG:Ce composite scintillator for x-ray imaging," Opt. Mater. **109**, 110305 (2020).
[59]R. T. Wegh, A. Meijerink, R.-J. Lamminmäki, and J. Hölsä, "Extending Dieke's diagram," J. Lumin. **87–89**, 1002–1004 (2000).
[60]S. Nargelas, M. Korjik, M. Vengris, and G. Tamulaitis, "Study of electronic excitation relaxation at cerium ions in $Gd_3Al_2Ga_3O_{12}$ matrix using multipulse transient absorption technique," J. Appl. Phys. **128**(10), 103104 (2020).
[61]K. Kamada, T. Endo, K. Tsutumi, T. Yanagida, Y. Fujimoto, A. Fukabori, A. Yoshikawa, J. Pejchal, and M. Nikl, "Composition engineering in cerium-doped $(Lu,Gd)_3(Ga,Al)_5O_{12}$ single-crystal scintillators," Cryst. Growth Des. **11**, 4484–4490 (2011).
[62]H. Wieczorek, V. Khanin, C. Ronda, J. Boerekamp, S. Spoor, R. Steadman, I. Venevtsev, K. Chernenko, T. Tukhvatulina, I. Vrubel, A. Meijerink, and P. Rodnyi, "Band gap variation and trap distribution in transparent garnet scintillator ceramics," IEEE Trans. Nucl. Sci. **67**(8), 1934–1945 (2020).
[63]W. Chewpraditkul, N. Pattanaboonmee, W. Chewpraditkul, T. Szczesniak, M. Moszynski, K. Kamada, A. Yoshikawa, R. Kucerkova, and M. Nikl, "Optical and scintillation properties of $LuGd_2Al_2Ga_3O_{12}$:Ce, $Lu_2GdAl_2Ga_3O_{12}$:Ce, and $Lu_2YAl_2Ga_3O_{12}$:Ce single crystals: A comparative study," Nucl. Instrum. Methods Phys. Res., Sect. A **1004**, 165381 (2021).

[64]X. Chen, H. Qin, Y. Zhang, Y. Liu, J. Jiang, and H. Jiang, "Microstructure and optical properties of transparent Nd:GAGG ceramics prepared via solid-state reactive sintering," Opt. Mater. Express **6**(2), 610 (2016).
[65]R. H. Lamoreaux, D. L. Hildenbrand, and L. Brewer, "High-temperature vaporization behavior of oxides II. Oxides of Be, Mg, Ca, Sr, Ba, B, Al, Ga, In, Tl, Si, Ge, Sn, Pb, Zn, Cd, and Hg," J. Phys. Chem. Ref. Data **16**(3), 419–443 (1987).
[66]N. Sakar, H. Gergeroglu, S. A. Akalin, S. Oguzlar, and S. Yildirim, "Synthesis, structural and optical characterization of Nd: YAG powders via flame spray pyrolysis," Opt. Mater. **103**, 109819 (2020).
[67]J. Marchal, T. John, R. Baranwal, T. Hinklin, and R. M. Laine, "Yttrium aluminum garnet nanopowders produced by liquid-feed flame spray pyrolysis (LF-FSP) of metalloorganic precursors," Chem. Mater. **16**(5), 822–831 (2004).
[68]M. Singlard, F. Rémondière, S. Oriol, G. Fiore, B. Vieille, M. Vardelle, and S. Rossignol, "Sol-gel synthesis of yttrium aluminum garnet (YAG): Effects of the precursor nature and concentration on the crystallization," J. Sol-Gel Sci. Technol. **87**(2), 496–503 (2018).
[69]P. Vaqueiro and M. A. López-quintela, "Synthesis of yttrium aluminium garnet by the citrate gel process," J. Mater. Chem. **8**(1), 161–163 (1998).
[70]P. Głuchowski, R. Tomala, R. Kowalski, O. Ignatenko, M. E. Witkowski, W. Drozdowski, W. Stręk, W. Ryba-Romanowski, and P. Solarz, "Frozen" pressure effect in GGAG:Ce^{3+} white light emitting nanoceramics," Ceram. Int. **45**(17), 21870–21877 (2019).
[71]J. Li, Y. Pan, F. Qiu, Y. Wu, and J. Guo, "Nanostructured Nd:YAG powders via gel combustion: The influence of citrate-to-nitrate ratio," Ceram. Int. **34**(1), 141–149 (2008).
[72]M. P. Pechini, U.S. patent 3330697A (11 July 1967).
[73]J.-G. Li, T. Ikegami, J.-H. Lee, and T. Mori, "Characterization of yttrium aluminate garnet precursors synthesized via precipitation using ammonium bicarbonate as the precipitant," J. Mater. Res. **15**(11), 2375–2386 (2000).
[74]Y. Zhang and H. Yu, "Synthesis of YAG powders by the co-precipitation method," Ceram. Int. **35**(5), 2077–2081 (2009).
[75]L. Wang, H. Kou, Y. Zeng, J. Li, Y. Pan, X. Sun, and J. Guo, "The effect of precipitant concentration on the formation procedure of yttrium aluminum garnet (YAG) phase," Ceram. Int. **38**(5), 3763–3771 (2012).
[76]P. Palmero and R. Traverso, "Co-precipitation of YAG powders for transparent materials: Effect of the synthesis parameters on processing and microstructure," Materials **7**(10), 7145–7156 (2014).
[77]X. Zhang, G. Yang, R. Chi, Y. Shi, X. Zhao, H. Jiang, F. Guo, G. Wang, J. Guo, and Z. Zhang, "Preparation of YAG nanopowders and ceramics via coprecipitation: Effects of treatment modes of precipitates," Int. J. Appl. Ceram. Technol. **19**(5), 2419–2426 (2022).
[78]Z. Hu, X. Chen, X. Liu, X. Li, T. Xie, Y. Shi, H. Kou, Y. Pan, E. Mihóková, M. Nikl, and J. Li, "Fabrication and scintillation properties of Pr:$Lu_3Al_5O_{12}$ transparent ceramics from co-precipitated nanopowders," J. Alloys Compd. **818**, 152885 (2020).
[79]Z. Wang, M. Xu, W. Zhang, and M. Yin, "Synthesis and luminescent properties of nano-scale LuAG:RE^{3+} (Ce, Eu) phosphors prepared by co-precipitation method," J. Lumin. **122–123**, 437–439 (2007).
[80]L. Pan, B. Jiang, J. Fan, P. Zhang, X. Mao, and L. Zhang, "Co-precipitation synthesis of lutetium aluminum garnet (LuAG) powders: The influence of ethanol," Opt. Mater. **71**, 50–55 (2017).
[81]Y. Wang, Z. Cheng, J. Ye, C. Hu, Z. Zhou, Y. Chen, H. Chen, D. Y. Kosyanov, and J. Li, "Ce:LuAG transparent ceramics for high-brightness solid-state lighting: Fabrication and effect of Ce concentration," Opt. Mater. **147**, 114697 (2024).
[82]D. Sun, Q. Zhang, Z. Wang, J. Su, C. Gu, A. Wang, and S. Yin, "Co-precipitation synthesis and sintering of nanoscaled Nd:$Gd_3Ga_5O_{12}$ polycrystalline material," Mater. Sci. Eng. A **392**(1–2), 278–281 (2005).
[83]Z. Luo, M. Lu, J. Bao, W. Liu, and C. Gao, "Co-precipitation synthesis of gadolinium gallium garnet powders using ammonium hydrogen carbonate as the precipitant," Mater. Lett. **59**(10), 1188–1191 (2005).
[84]L. Science and D. Technology Centre, "Nd:GGG nanopowders by microwave gel combustion route and sinterability studies," Def. Sci. J. **64**(5), 490–494 (2014).
[85]Y. Sun, S. Yang, Y. Zhang, J. Jiang, and H. Jiang, "Co-precipitation synthesis of gadolinium aluminum gallium oxide (GAGG) via different precipitants," IEEE Trans. Nucl. Sci. **61**(1), 306–311 (2014).
[86]S. Yang, Y. Sun, X. Chen, Y. Zhang, Z. Luo, J. Jiang, and H. Jiang, "The effects of cation concentration in the salt solution on the cerium doped gadolinium gallium aluminum oxide nanopowders prepared by a Co-precipitation method," IEEE Trans. Nucl. Sci. **61**(1), 301–305 (2014).
[87]Z. Luo, H. Jiang, J. Jiang, and R. Mao, "Microstructure and optical characteristics of Ce:$Gd_3(Ga,Al)_5O_{12}$ ceramic for scintillator application," Ceram. Int. **41**(1), 873–876 (2015).
[88]J.-Y. Zhang, Z.-H. Luo, H.-C. Jiang, J. Jiang, C.-H. Chen, J.-X. Zhang, Z.-Z. Gui, and N. Xiao, "Highly transparent cerium doped gadolinium gallium aluminum garnet ceramic prepared with precursors fabricated by ultrasonic enhanced chemical co-precipitation," Ultrason. Sonochem. **39**, 792–797 (2017).
[89]L. V. Ermakova, V. G. Smyslova, V. V. Dubov, P. V. Karpyuk, P. S. Sokolov, I. Y. Komendo, A. G. Bondarau, V. A. Mechinsky, and M. V. Korzhik, "Scintillation and luminescent properties of the $(Gd,Y)_3Al_2Ga_3O_{12}$:Ce ceramics obtained by compaction of green bodies using digital light processing 3D printing," Photonics **11**(8), 695 (2024).
[90]X. Li and Q. Li, "YAG ceramic processed by slip casting via aqueous slurries," Ceram. Int. **34**(2), 397–401 (2008).
[91]Z. M. Seeley, N. J. Cherepy, and S. A. Payne, "Homogeneity of Gd-based garnet transparent ceramic scintillators for gamma spectroscopy," J. Cryst. Growth **379**, 79–83 (2013).
[92]Q. Yao, L. Zhang, P. Gao, B. Sun, C. Shao, Y. Ma, T. Zhou, M. Li, H. Chen, and Y. Wang, "Viscoelastic behaviors and drying kinetics of different aqueous gelcasting systems for large Nd: YAG laser ceramics rods," J. Am. Ceram. Soc. **103**(6), 3513–3527 (2020).
[93]X. Ba, J. Li, Y. Pan, Y. Zeng, H. Kou, W. Liu, J. Liu, L. Wu, and J. Guo, "Comparison of aqueous- and non-aqueous-based tape casting for preparing YAG transparent ceramics," J. Alloys Compd. **577**, 228–231 (2013).
[94]J.-Y. Zhang, Z.-H. Luo, H.-C. Jiang, J. Jiang, Z.-Z. Gui, C.-H. Chen, Y.-F. Liu, S. Liu, and M.-M. Ci, "Sintering of GGAG:Ce^{3+}, xY^{3+} transparent ceramics in oxygen atmosphere," Ceram. Int. **43**(17), 16036–16041 (2017).
[95]S. Hu, Y. Liu, Y. Zhang, Z. Xue, Z. Wang, G. Zhou, C. Lu, H. Li, and S. Wang, "3D printed ceramic phosphor and the photoluminescence property under blue laser excitation," J. Eur. Ceram. Soc. **39**(8), 2731–2738 (2019).
[96]Y. Shi, Y. Zhao, M. Cao, H. Chen, Z. Hu, X. Chen, Z. Zhang, and Q. Liu, "Dense Ce^{3+} doped $Lu_3A1_5O_{12}$ ceramic scintillators with low sintering adds: Doping content effect, luminescence characterization and proton irradiation hardness," J. Lumin. **225**, 117336 (2020).
[97]S. Chen, B. Jiang, Q. Zhu, W. Ma, G. Zhang, Y. Jiang, W. Chewpraditkul, and L. Zhang, "Effect of annealing atmosphere on scintillation properties of GYGAG: Ce, Mg scintillator ceramics," Nucl. Instrum. Methods Phys. Res., Sect. A **942**, 162360 (2019).
[98]X. Chen, X. Liu, Y. Feng, X. Li, H. Chen, T. Xie, H. Kou, R. Kučerková, A. Beitlerová, E. Mihóková, M. Nikl, and J. Li, "Microstructure evolution in two-step-sintering process toward transparent Ce:$(Y,Gd)_3(Ga,Al)_5O_{12}$ scintillation ceramics," J. Alloys Compd. **846**, 156377 (2020).
[99]X. Qiu, Z. Luo, J. Zhang, H. Jiang, and J. Jiang, "Mechanical properties and machinability of GYGAG:Ce ceramic scintillators," Ceram. Int. **46**(4), 4550–4555 (2020).
[100]R. Boulesteix, A. Maître, J.-F. Baumard, C. Sallé, and Y. Rabinovitch, "Mechanism of the liquid-phase sintering for Nd:YAG ceramics," Opt. Mater. **31**(5), 711–715 (2009).
[101]S. Lee, E. R. Kupp, A. J. Stevenson, J. M. Anderson, G. L. Messing, X. Li, E. C. Dickey, J. Q. Dumm, V. K. Simonaitis-Castillo, and G. J. Quarles, "Hot isostatic pressing of transparent Nd:YAG ceramics," J. Am. Ceram. Soc. **92**(7), 1456–1463 (2009).
[102]A. J. Stevenson, E. R. Kupp, and G. L. Messing, "Low temperature, transient liquid phase sintering of B_2O_3–SiO_2 -doped Nd:YAG transparent ceramics," J. Mater. Res. **26**(9), 1151–1158 (2011).

[103]G. Zhang, D. Carloni, and Y. Wu, "3D printing of transparent YAG ceramics using copolymer-assisted slurry," Ceram. Int. **46**(10), 17130–17134 (2020).

[104]Y. Zhang, S. Hu, Z. Wang, G. Zhou, and S. Wang, "Pore-existing $Lu_3Al_5O_{12}$: Ce ceramic phosphor: An efficient green color converter for laser light source," J. Lumin. **197**, 331–334 (2018).

[105]X. Chen, H. Qin, Y. Zhang, J. Jiang, and H. Jiang, "Highly transparent ZrO_2-doped $(Ce,Gd)_3Al_3Ga_2O_{12}$ ceramics prepared via oxygen sintering," J. Eur. Ceram. Soc. **35**(14), 3879–3883 (2015).

[106]X. Huang, J. He, Y. Jiang, W. Chewpraditkul, and L. Zhang, "Ultrafast GGAG:Ce x-ray scintillation ceramics with Ca^{2+} and Mg^{2+} co-dopants," Ceram. Int. **48**(16), 23571–23577 (2022).

[107]P. Prusa, M. Kučera, V. Babin, P. Bruza, T. Parkman, D. Panek, A. Beitlerova, J. A. Mares, M. Hanus, Z. Lucenicova, M. Pokorny, and M. Nikl, "Tailoring and optimization of LuAG:Ce epitaxial film scintillation properties by Mg Co-doping," Cryst. Growth Des. **18**(9), 4998–5007 (2018).

[108]J. N. Song, B. H. Bae, K. H. Hu, H. Lee, H.-D. Jung, and C.-B. Yoon, "Effects of tetraethyl orthosilicate content and sintering temperature on the properties of $Y_3Al_5O_{12}$:Ce^{3+} phosphor ceramics for automotive headlamps," Mater. Today Commun. **28**, 102473 (2021).

[109]M. Mori, J. Xu, G. Okada, T. Yanagida, J. Ueda, and S. Tanabe, "Comparative study of optical and scintillation properties of Ce:YAGG, Ce:GAGG and Ce: LuAGG transparent ceramics," J. Ceram. Soc. Jpn. **124**(5), 569–573 (2016).

[110]P. Karpyuk, A. Shurkina, D. Kuznetsova, V. Smyslova, V. Dubov, G. Dosovitskiy, M. Korzhik, V. Retiviv, and A. Bondarev, "Effect of sintering additives on the sintering and spectral-luminescent characteristics of quaternary GYAGG:Ce scintillation ceramics," J. Electron. Mater. **51**(11), 6481–6491 (2022).

[111]T. K. Lewellen, "Time-of-flight PET," Semin. Nucl. Med. **28**(3), 268–275 (1998).

[112]N. A. Laishevceva, E. V. Tkachenko, and V. D. Juravlev, "The system of $PbWO_4$–$SrWO_4$," Russ. J. Inorg. Chem. **28**(12), 3137–3140 (1983).

[113]A. Lempicki, E. Berman, A. J. Wojtowicz, M. Balcerzyk, and L. A. Boatner, "Cerium-doped orthophosphates: New promising scintillators," IEEE Trans. Nucl. Sci. **40**(4), 384–387 (1993).

[114]A. J. Wojtowicz, A. Lempicki, D. Wisniewski, and L. A. Boatner, "Cerium-doped orthophosphate scintillators," MRS Proc. **348**, 123–129 (1994).

[115]P. Dorenbos, "The electronic level structure of lanthanide impurities in $REPO_4$, $REBO_3$, $REAlO_3$, and RE_2O_3 (RE = La, Gd, Y, Lu, Sc) compounds," J. Phys.: Condens. Matter **25**(22), 225501 (2013).

[116]V. Vistovskyy, T. Malyy, A. Pushak, A. Vas'kiv, A. Shapoval, N. Mitina, A. Gektin, A. Zaichenko, and A. Voloshinovskii, "Luminescence and scintillation properties of $LuPO_4$–Ce nanoparticles," J. Lumin. **145**, 232–236 (2014).

[117]D. Spassky, V. Voznyak-Levushkina, A. Arapova, B. Zadneprovski, K. Chernenko, and V. Nagirnyi, "Enhancement of light output in $Sc_xY_{1-x}PO_4$: Eu^{3+} solid solutions," Symmetry **12**(6), 946 (2020).

[118]D. Spassky, A. Vasil'ev, V. Nagirnyi, I. Kudryavtseva, D. Deyneko, I. Nikiforov, I. Kondratyev, and B. Zadneprovski, "Bright UV-C phosphors with excellent thermal stability—$Y_{1-x}Sc_xPO_4$ solid solutions," Materials **15**(19), 6844 (2022).

[119]A. Syntfeld, M. Moszynski, R. Arlt, M. Balcerzyk, M. Kapusta, M. Majorov, R. Marcinkowski, P. Schotanus, M. Swoboda, and D. Wolski, "^{6}LiI(Eu) in neutron and gamma-ray spectrometry-a highly sensitive thermal neutron detector," IEEE Trans. Nucl. Sci. **52**(6), 3151–3156 (2005).

[120]A. Fedorov, V. Gurinovich, V. Guzov, G. Dosovitskiy, M. Korzhik, V. Kozhemyakin, A. Lopatik, D. Kozlov, V. Mechinsky, and V. Retivov, "Sensitivity of GAGG based scintillation neutron detector with SiPM readout," Nucl. Eng. Technol. **52**(10), 2306–2312 (2020).

[121]E. V. D. Van Loef, J. Glodo, W. M. Higgins, and K. S. Shah, "Optical and scintillation properties of Cs_2LiYCl_6:Ce^{3+} and Cs_2LiYCl_6:Pr^{3+} crystals," IEEE Trans. Nucl. Sci. **52**(5), 1819–1822 (2005).

[122]A. Bessiere, P. Dorenbos, C. W. E. Van Eijk, K. W. Kramer, and H. U. Gudel, "New thermal neutron scintillators: Cs_2LiYCl_6:Ce^{3+} and Cs_2LiYBr_6:Ce^{3+}," IEEE Trans. Nucl. Sci. **51**(5), 2970–2972 (2004).

[123]M. Moszynski, M. Balcerzyk, M. Kapusta, A. Syntfeld, D. Wolski, G. Pausch, J. Stein, and P. Schotanus, "$CdWO_4$ crystal in gamma-ray spectrometry," IEEE Trans. Nucl. Sci. **52**(6), 3124–3128 (2005).

[124]P. G. Koontz, G. R. Keepin, and J. E. Ashley, "ZnS(Ag) phosphor mixtures for neutron scintillation counting," Rev. Sci. Instrum. **26**(4), 352–356 (1955).

[125]H. Pan, Q. Liu, X. Chen, X. Liu, H. Chen, T. Xie, W. Wang, Y. Shi, X. Jiang, J. Zhou, Z. Sun, M. Nikl, and J. Li, "Fabrication and properties of Gd_2O_2S:Tb scintillation ceramics for the high-resolution neutron imaging," Opt. Mater. **105**, 109909 (2020).

[126]E. V. D. Van Loef, L. P. Dorenbos, C. W. E. Van Eijk, K. Kramer, and H. U. Gudel, "Scintillation properties of $LaCl_3$:Ce^{3+} crystals: Fast, efficient, and high-energy resolution scintillators," IEEE Trans. Nucl. Sci. **48**(3), 341–345 (2001).

[127]R. C. Murty, "Effective atomic numbers of heterogeneous materials," Nature **207**(4995), 398–399 (1965).

[128]Y. Fujimoto, K. Kamada, T. Yanagida, N. Kawaguchi, S. Kurosawa, D. Totsuka, K. Fukuda, K. Watanabe, A. Yamazaki, Y. Yokota, and A. Yoshikawa, "Lithium aluminate crystals as scintillator for thermal neutron detection," IEEE Trans. Nucl. Sci. **59**(5), 2252–2255 (2012).

[129]Q. Wu, J. Ding, Y. Li, X. Wang, and Y. Wang, "$LiCaAlN_2$:Eu^{3+}/Tb^{3+}: Red and green phosphors for LEDs and FEDs with charge transfer transition in n-UV region," J. Am. Ceram. Soc. **100**(7), 3088–3098 (2017).

[130]I. Komendo, A. Bondarev, A. Fedorov, G. Dosovitskiy, V. Gurinovich, D. Kazlou, V. Kozhemyakin, V. Mechinsky, A. Mikhlin, V. Retivov, V. Schukin, A. Timochenko, M. Murashev, A. Zharova, and M. Korzhik, "New scintillator $6Li_2CaSiO_4$:Eu^{2+} for neutron sensitive screens," Nucl. Instrum. Methods Phys. Res., Sect. A **1045**, 167637 (2023).

[131]I. Komendo, V. Mechinsky, A. Fedorov, G. Dosovitskiy, V. Schukin, D. Kuznetsova, M. Zykova, Y. Velikodny, and M. Korjik, "Effect of the synthesis conditions on the morphology, luminescence and scintillation properties of a new light scintillation material Li_2CaSiO_4:Eu^{2+} for neutron and charged particle detection," Inorganics **10**(9), 127 (2022).

[132]M. Y. Sharonov, A. B. Bykov, V. Petričević, and R. R. Alfano, "Cr^{4+}-doped Li_2CaSiO_4 crystal: Growth and spectroscopic properties," Opt. Commun. **231**(1–6), 273–280 (2004).

[133]V. Smyslova, D. Kuznetsova, A. Bondaray, P. Karpyuk, M. Korzhik, I. Komendo, V. Pustovarov, V. Retivov, and D. Tavrunov, "Advances of the cubic symmetry crystalline systems to create complex, bright luminescent ceramics," Photonics **10**(5), 603 (2023).

[134]A. Nepomnyashchikh, E. Radzhabov, A. Egranov, and V. Ivashechkin, "Luminescence of BaF_2–LaF_3," Radiat. Meas. **33**, 759–762 (2001).

[135]S. Otake, T. Kato, D. Nakauchi, N. Kawaguchi, and T. Yanagida, "Development of Eu:BaFCl translucent ceramic scintillators," J. Lumin. **275**, 120828 (2024).